LWI Bericht Nr. 943

Permeability of GSC-Structures
-Laboratory Tests and Results-

DAAD Stipendiat M.Sc. Juan Recio
Professor Dr.-Ing. Hocine Oumeraci

BRAUNSCHWEIG
May 2007

Table of Contents   Page

Permeability of GSC-Structures:
Laboratory Tests and Results

The permeability of coastal structures such as revetments, seawalls, breakwaters, etc. significantly affects their hydraulic stability when subject to wave loads (e. g. Hendar 1960, Hudson 1959 and 1961, Pilarcyzck 1998). The higher the permeability of a revetment, the higher its stability. Higher permeability reduces the seepage forces and pressure "build-up" in the structure. Permeability also strongly affects wave transmission and other processes associated with wave-structure interaction (Chao-Lung, 2004; and Muttray and Oumeraci, 2002). In addition, permeability is extremely important for GSC-structures used as flood defences (e.g. dune reinforcement, seawalls, etc.), since it substantially affects the inundation rate. Despite the importance of the permeability for both functional design and hydraulic stability, no information is available for the assessment of the permeability of GSC-structures.

Therefore, comprehensive hydraulic model tests have been performed for the first time to determine the permeability of several types of GSC-structures. Moreover, the stability of GSC-structures having different permeability and different mode of placement of the sand containers but same geometry is investigated under wave action in the wave-flume of Leichtweiss Institute (LWI). Finally, a conceptual model for the permeability of GSC-structures is proposed.

1.Theoretical Background

The two most common approaches to describe the flow through porous structures are those proposed by Darcy and Forchheimer.

 If the flow through the structure is **steady and laminar,** Darcy's formula (Lambe 1979) can be used (Figure 1):

$$Q = k \, i \, A \qquad (1)$$

where Q is the flow rate; k the Darcy's coefficient of permeability (depends on the soil and viscosity of the pore fluid); A is the total cross area of filter sample normal to the flow and i is the hydraulic gradient:

$$i = \frac{\Delta h}{\Delta l} = const \qquad (2)$$

with Δh is water head difference, before and after the filter sample ($\Delta h = h_1 - h_2$) and Δl is the length of filter sample.
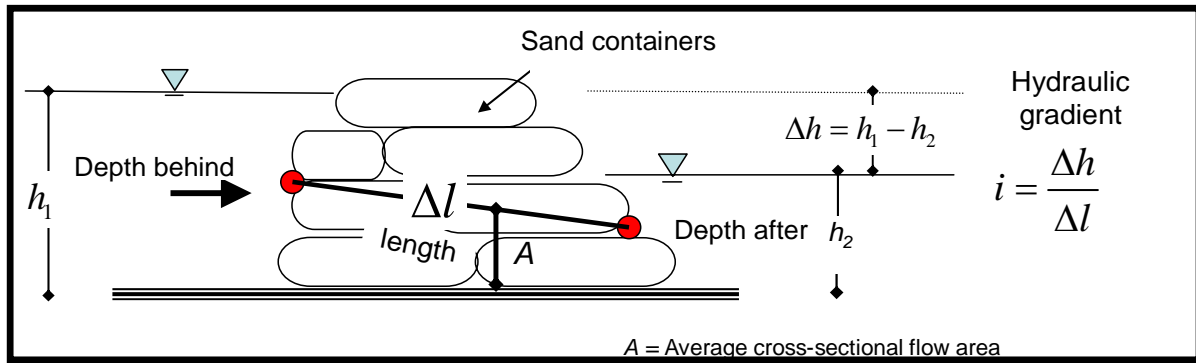
Figure 1: Flow through GSC-Structures

If the flow through the structure is **unsteady and turbulent**, i. e. when the Reynolds number *Re* and the inertia of the fluid on the grain particles become important, the Darcy relation can no longer be expressed in a linear form. For these cases the approach suggested by Forcheimer would rather apply (Engelund 1953):

$$i = au + bu^2 \qquad\qquad (3)$$

where *a* and *b* are two empirical coefficients which can be expressed as:

$$a = \alpha \frac{(1-n)^3}{n^2} \frac{v}{gD^2} \qquad\qquad (4)$$

$$b = \beta \frac{(1-n)}{n^3} \frac{1}{gD} \qquad\qquad (5)$$

where *n* is the porosity of the material, *g* is the acceleration of gravity, *D* the diameter of the grain, *v* is the kinematics viscosity of water and α and β are empirical coefficients.

The flow through a GSC-structure is not homogeneous. Turbulent flow is expected to occur in the gaps between containers, but the rest of the flow is expected to be laminar. Despite the in-homogeneity of the flow and its unsteadiness, the permeability of GSC-structure will preferably be described by the Darcy permeability coefficient *k*.

2. Basic Permeability Tests for GSC-Structures.
Permeability tests were performed to obtain the permeability of various types of GSC-structures and to quantify the influence of parameters such as the size of the containers, the gap size and the mode of placement of GSCs on the permeability.

2.1 Experimental Set-Up
The permeability tests were performed by constructing a GSC-structure in a tank (2m wide, 5m long and 1.5m high). The height of GSC-structure is 1.3m, width 2m and variable length depending on the model. The water head difference was kept constant during each test in order to ensure steady flow conditions (Figure 2). Several structure geometries and two sizes of sand containers were tested under at least three different hydraulic gradients (Figure 3).

The **measurements** during the model tests focused on the in-outflow (Figure 2). These were obtained by means of ADV-devices (**A**coustic **D**oppler **V**elocimeters). The ADVs were located 0.11m from the structure, exactly faced to a gap between containers (closest possible location). The water depths at both side of the structure and the steady flow were also recorded.
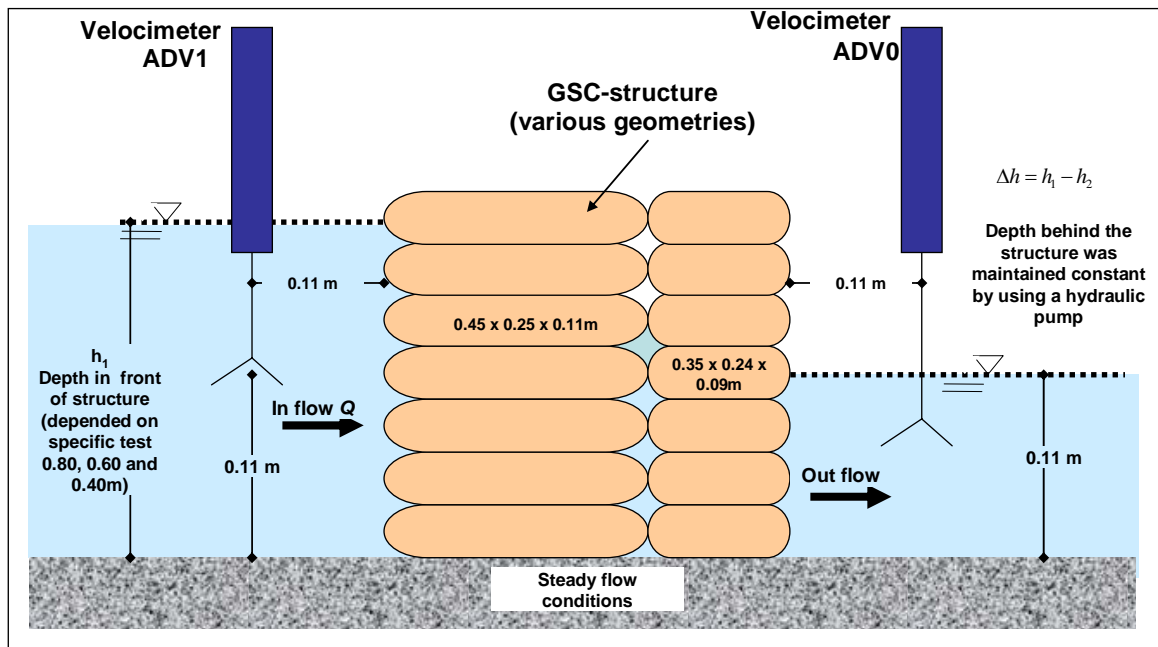
Figure 2: Experimental Set-Up for Basic Permeability Tests

The sand containers used in the model tests were made of a nonwoven geotextile with a permeability coefficient of k= 1.1 x 10^{-1} m/s and sand with a median grain size of D_{50}= 0.2mm, density of ρ_s =1800 kg/m^3 and permeability coefficient of approx k= 1.1 x 10^{-4} m/s (Table 1).

Table 1. Properties of the Geotextile used as Container (secutex GRK 150g/m^2) (After Naue, 2004)

Description	Test Procedure	Unit	Value
Mass per Area	DIN EN 965	g/m^2	150
Thickness	DIN EN 964-1	Mm	1.8
Tensile strength (machine direction/ trans)	DIN EN ISO 10319	kN/m	6.0/11.0
Penetration Test	DIN EN ISO 12236	N	1.670
Deformation by Penetration Test	DIN EN ISO 12956	%	35
Permeability VI$_{H50}$ Index	DIN EN ISO 11058	m/s	1.1 x 10^{-1}
Permeability Flow rate$_{H50}$	DIN EN ISO 11058	l/sm^2	110
Transmitivity by 2 kPa	DIN EN ISO 12958	m^2/s	4.5 x 10^{-5}
Characteristic Opening Size	DIN EN ISO 12956	mm	0.13

The sand containers have a filling ratio of 80%. Two sizes of sand containers were used (Figure 3): (i) 0.45m x 0.28m x 0.11m and (ii) 0.35m x 0.24m x 0.09m.
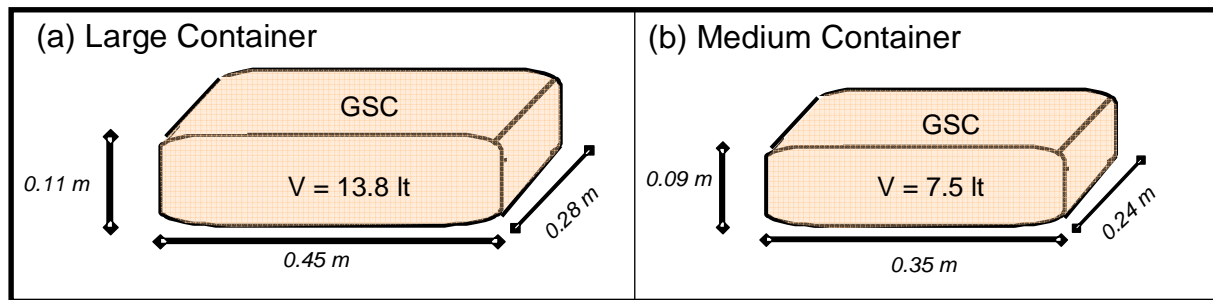
Figure 3: Sizes of Containers Used in the Permeability Model Tests

A total of 11 model alternatives were tested (Figure 4), which differ from each other by the following items: (i) lay-out of the containers in the arrangement of the structure, (ii) size of containers and (iii) length of the structure.
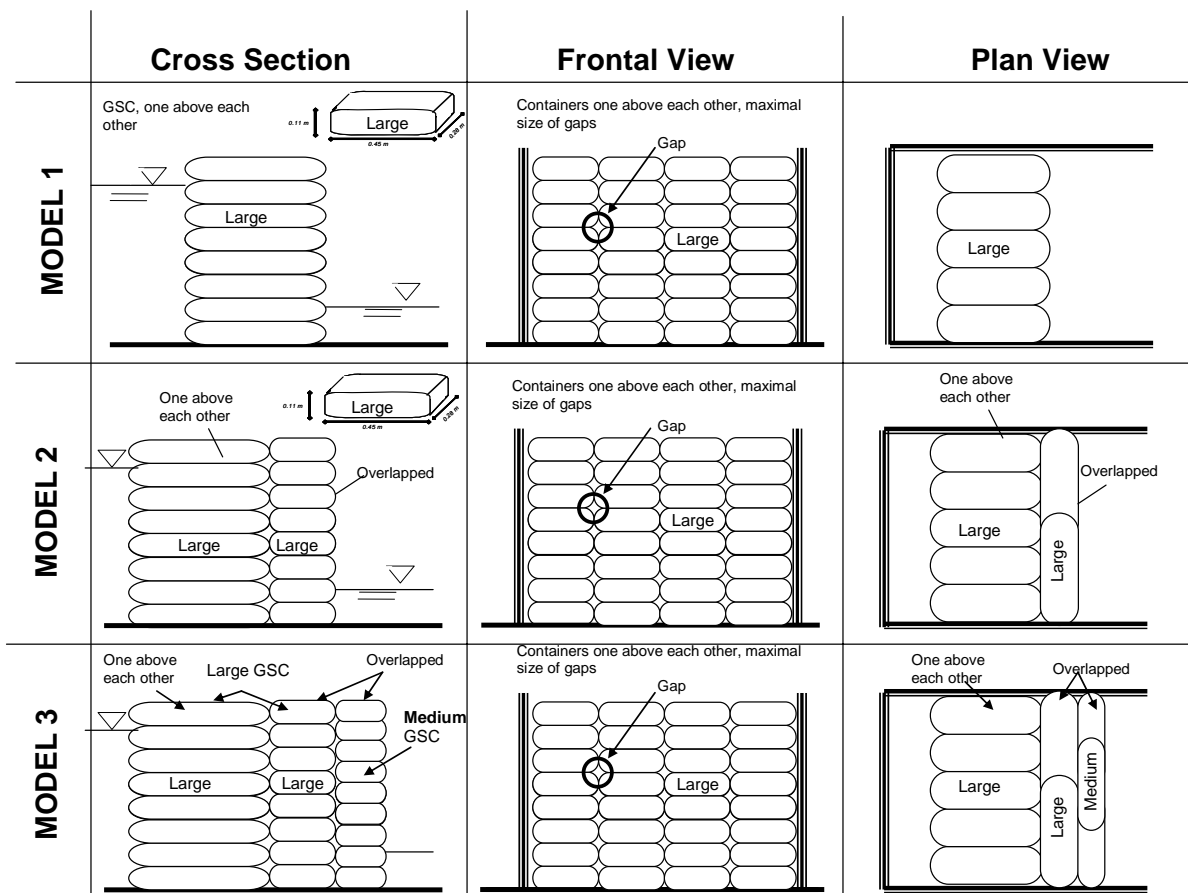
Figure 4: Model Alternatives Considered in Basic Permeability Tests (continues on next page)
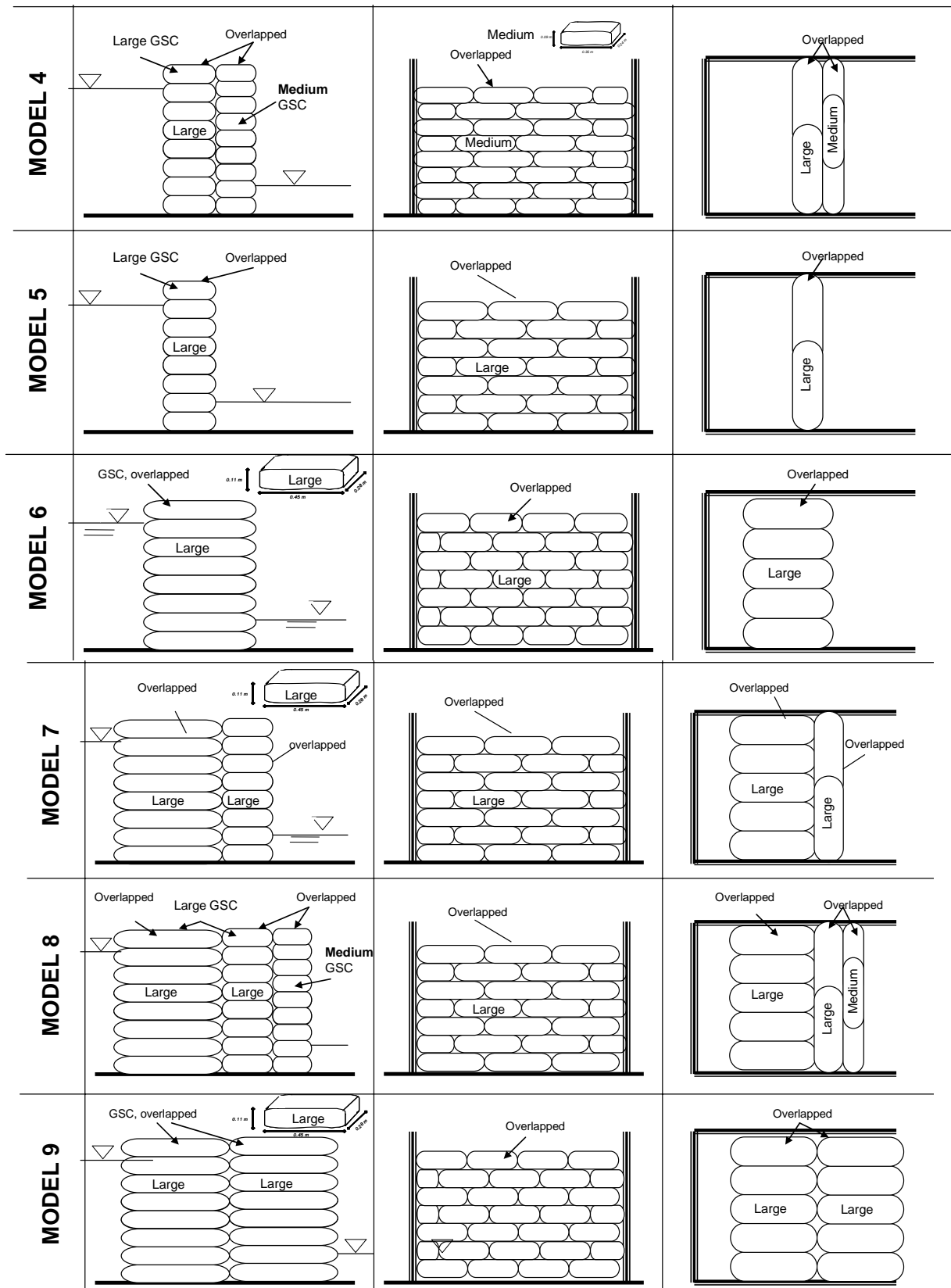
Figure 4 : Model Alternatives Considered in Basic Permeability Tests (continues on next page)
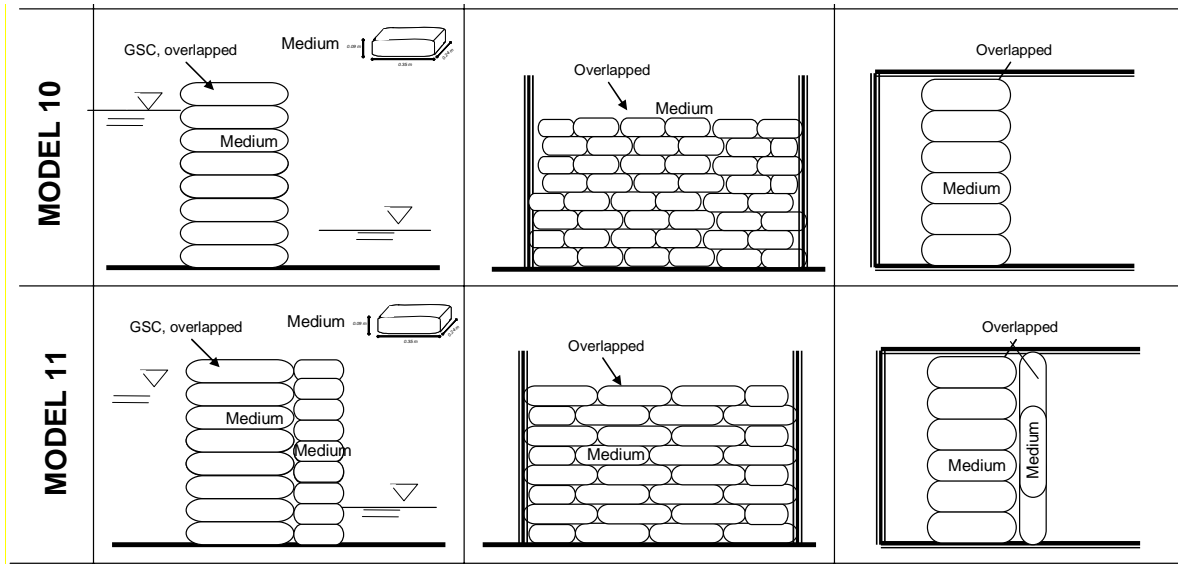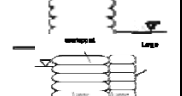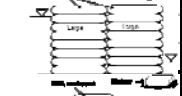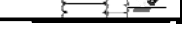
Figure 4: Model Alternatives Considered in Basic Permeability Tests (continued from previous page)

2.2 Results of Basic Permeability Tests

The definition of the parameters used and the results of the permeability tests are summarized in Figure 1 and Table 2, respectively.

To investigate the influence of the size of the gaps between GSCs and other parameters such as the size of container and arrangement of GSCs, a comparative analysis of the results was performed.

![LWI logo] Permeability of GSC-Structures

Table 2: Results of Basic Permeability Tests

Nr.	Cross Section	Test No.	Model	h1 (m)	h2 (m)	L (m)	Δl (m)	i	A (m2)	Q (m3/s)	Q (l/s)	ADV vel (cm/s)	k (m/s)	k AVG (m/s)
1		1a	1	0.47	0.11	0.50	0.59	0.61	0.35	0.0113	11.25	17.23	0.0531	
		1b	1	0.47	0.11	0.50	0.59	0.61	0.35	0.0107	10.74	18.02	0.0507	0.050
		1c	1	0.52	0.11	0.50	0.58	0.71	0.38	0.0139	13.94	xx	0.0520	
2		2a	2	0.43	0.11	0.80	0.87	0.37	0.32	0.0021	2.07	1.79	0.0173	
		2b	2	0.50	0.11	0.80	0.85	0.46	0.37	0.0039	3.88	3.45	0.0232	0.020
		2c	2	0.47	0.11	0.80	0.86	0.42	0.35	0.0032	3.21	3.72	0.0220	
		2d	2	0.42	0.11	0.80	0.87	0.36	0.32	0.0046	4.61	2.77	0.0407	
3		3a	3	0.57	0.11	1.15	1.18	0.39	0.41	0.0018	1.81	2.69	0.0114	
		3b	3	0.42	0.11	1.15	1.20	0.26	0.32	0.0013	1.34	xx	0.0164	0.013
		3c	3	0.45	0.11	1.15	1.20	0.28	0.34	0.0012	1.19	xx	0.0125	
4		4a	4	0.52	0.11	0.56	0.63	0.65	0.38	0.0014	1.37	1.05	0.0056	
		4b	4	0.47	0.11	0.56	0.64	0.56	0.35	0.0013	1.25	1.90	0.0064	0.005
		4c	4	0.40	0.11	0.56	0.66	0.44	0.31	0.0010	1.00	xx	0.0055	
		4d	4	0.54	0.11	0.56	0.63	0.69	0.39	0.0016	1.55	1.29	0.0058	
5		5a	5	0.52	0.11	0.32	0.43	0.95	0.38	0.0029	2.91	7.47	0.0081	
		5b	5	0.46	0.11	0.32	0.45	0.77	0.34	0.0022	2.15	3.29	0.0081	0.008
		5c	5	0.39	0.11	0.32	0.48	0.59	0.30	0.0014	1.39	xx	0.0079	
6		6a	6	0.43	0.11	0.50	0.60	0.53	0.32	0.0028	2.80	5.42	0.0163	
		6b	6	0.52	0.11	0.50	0.58	0.71	0.38	0.0038	3.85	6.15	0.0144	0.015
		6c	6	0.47	0.11	0.50	0.59	0.61	0.35	0.0029	2.93	4.86	0.0138	
7		7a	7	0.55	0.11	0.80	0.85	0.52	0.40	0.0020	1.98	2.51	0.0096	
		7b	7	0.42	0.11	0.80	0.87	0.36	0.32	0.0011	1.09	2.02	0.0096	0.009
		7c	7	0.48	0.11	0.80	0.86	0.43	0.35	0.0023	2.29	2.42	0.0150	
8		8a	8	0.46	0.11	1.10	1.15	0.31	0.34	0.0011	1.12	xx	0.0107	
		8b	8	0.43	0.11	1.10	1.15	0.28	0.32	0.0009	0.93	1.54	0.0103	0.010
		8c	8	0.48	0.11	1.10	1.14	0.32	0.35	0.0011	1.08	xx	0.0094	
9		9a	9	0.48	0.11	1.00	1.05	0.35	0.35	0.0019	1.92	3.52	0.0153	
		9b	9	0.42	0.11	1.00	1.06	0.29	0.32	0.0014	1.37	4.69	0.0147	0.014
		9c	9	0.45	0.11	1.00	1.05	0.32	0.34	0.0015	1.54	xx	0.0142	
10		10a	10	0.47	0.11	0.45	0.55	0.66	0.35	0.0019	1.87	xx	0.0082	
		10b	10	0.39	0.11	0.45	0.57	0.49	0.30	0.0012	1.21	2.84	0.0082	0.008
		10c	10	0.52	0.11	0.45	0.54	0.77	0.38	0.0024	2.37	3.01	0.0082	
11		11a	11	0.51	0.11	0.75	0.81	0.50	0.37	0.0013	1.35	3.49	0.0073	
		11b	11	0.48	0.11	0.75	0.81	0.46	0.35	0.0012	1.16	2.87	0.0072	0.007
		11c	11	0.44	0.11	0.75	0.82	0.40	0.33	0.0010	0.98	2.56	0.0074	
									AVG= average			xx= value not measured		

2.2.1 Effect of the Size of the Gaps between Containers on Permeability

The first parameter that was investigated was the size of the gaps between neighbouring containers. Therefore, two GSC-structures with the same containers but different gap size between GSCs were compared. By laying the containers one directly above the other, the size of the gaps becomes maximum. On the other hand, if the GSC are laid with some interlocking, the size of the gaps is reduced (but more gaps will be present).
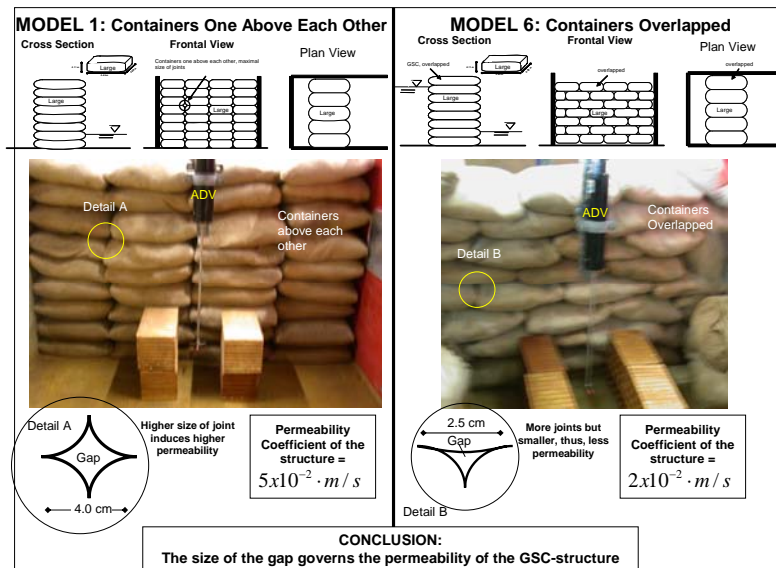
Figure 5: Effect of Size of Gaps on the Permeability of GSC-Structures

The size of the gaps substantially affect the permeability of GSC-structures. The difference between the permeability coefficients of the two GSC-arrangements in Figure 5 is more than twice (k= 5 x 10^{-2} to 2 x 10^{-2}m/s).

It was also observed that with a big size of gaps, the flow velocities through the gaps are very high (Figure 6).
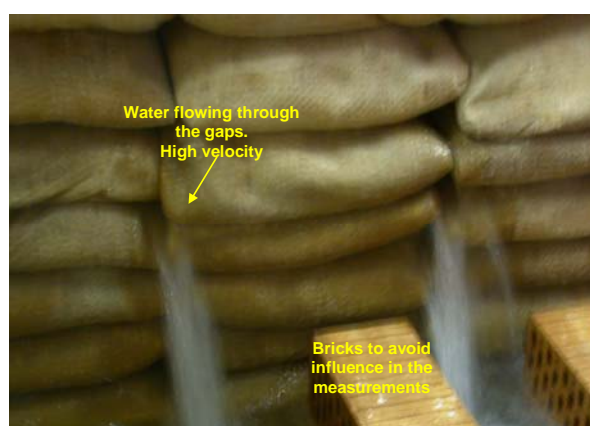
Figure 6: Close-Up of the Flow through the Gaps During the Tests (model 1)

From this analysis it can be concluded that:
- The main flow through GSC-structures is through the gaps, and
- For GSC-structures, the size of the gap governs the overall permeability of the GSC-structure.

2.2.2. Effect of Size of Container on Permeability

In order to investigate the influence of the size of the containers on the permeability of GSC-structures, two containers with different size were tested under same flow conditions. The comparative results are summarized in Figure 8 showing that:

- The size of the container influences the permeability of structure.
- The smaller the container, the smaller the permeability coefficient of the structure. This can be explained due to the size of gaps between containers. A structure built with smaller containers will have more gaps but the size of these gaps is smaller. This indicates that the friction between flow and the geotextile in the gaps is high and reduces considerably the flow through the structure. In example, the flow through a single gap with an area of 2 units is higher than the total flow through two gaps having each of them an area of one unit (due to the friction between geotextile and water) (Figure 7).
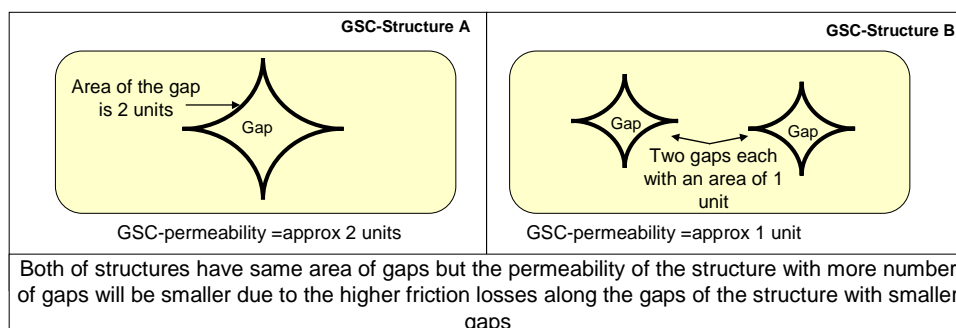
Figure 7: Influence of the Size of the Gap on the Permeability
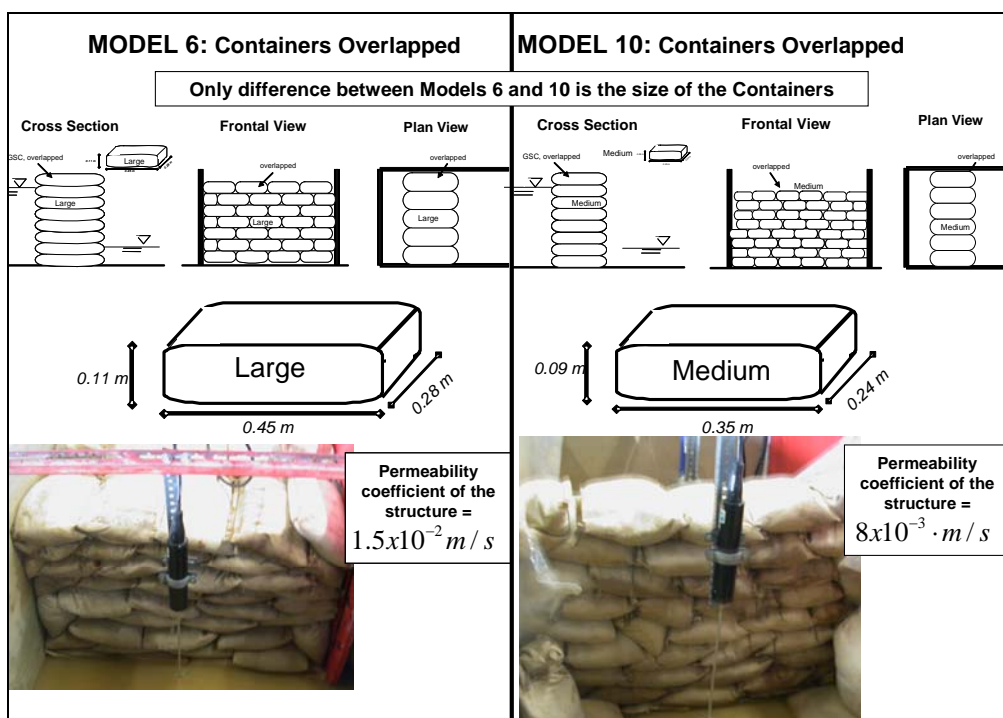
Figure 8: Effect of Size of the Container on the Permeability of GSC-Structures (continues in next page)
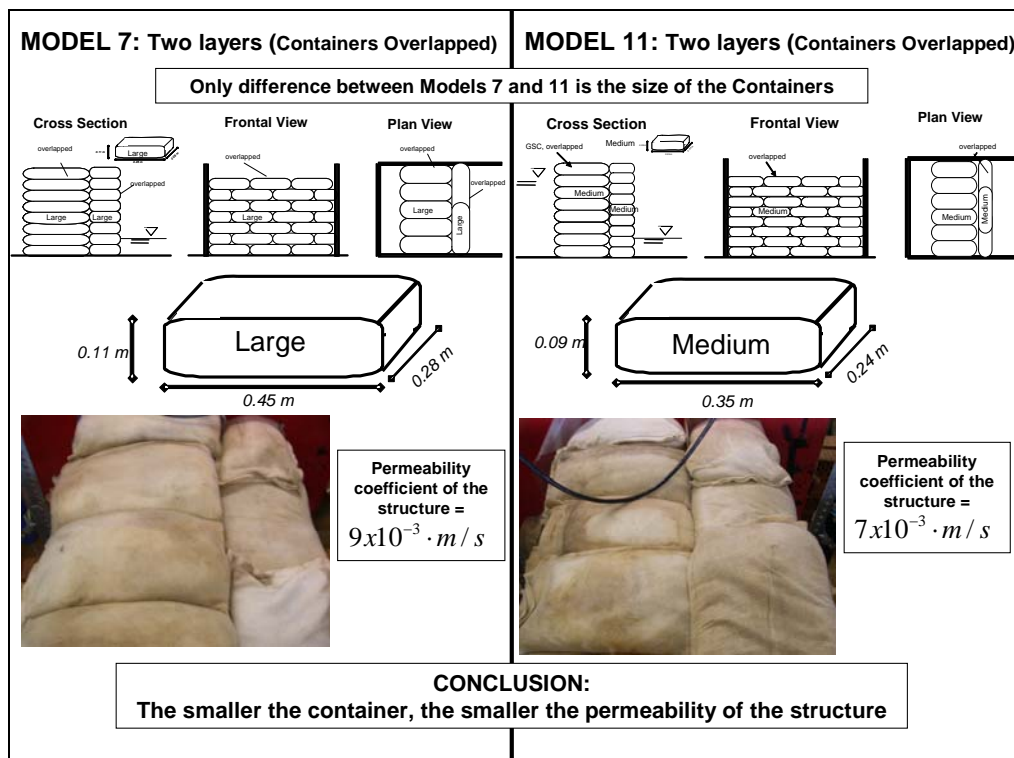
Figure 8: Effect of Size of the Container on the Permeability of GSC-structures (continued from previous page)

2.2.3. Effect of GSC-Arrangement on Permeability

A structure with longitudinal palced GSCs (in Plan view) is compared with a structure with transversally placed GSCs (Figure 9).

Recalling that the permeability coefficient in Darcy's formula (eq. 1 and 2) is inversely proportional to the length of the structure (Δl), a shorter structure has a smaller permeability coefficient. But comparing the flow behind the structure, it can be seen that the flow is similar in both cases (slightly higher flow with shorter structures, see aslo Table 2).

If we consider that both structures were built with identical containers, then the size of the gaps between containers should be the same. From the analysis it can be stated that a longitudinal structure has less gaps but the length of these gaps is longer. On the other hand, transversal structures have fewer gaps but shorter.

MODEL 6: One longitudinal layer (in plan view) of containers

Permeability coefficient of the structure = $1.4x10^{-2}\,m/s$

MODEL 5: One transversal layer of containers (in plan view)

Permeability coefficient of the structure = $8x10^{-3} \cdot m/s$

MODEL 9: Two longitudinal layers of containers

Permeability coefficient of the structure = $1.4x10^{-2} \cdot m/s$

MODEL 4: Two transversal layers of containers

Permeability coefficient of the structure = $6x10^{-3} \cdot m/s$

CONCLUSION:
Longitudinal containers have higher permeability then transversal (less number of gaps)

Figure 9: Effect of Mode of Placement of Containers on the Permeability of GSC-Structures

From this comparison it can be concluded that:
- Transversally placed GSCs have smaller permeability coefficients than longitudinally placed GSCs.
- If only the permeability of the structure is important, then both longitudinal or traversally placed GSCs will provide similar total flows through the structure. However, the hydraulic stability of sand containers under wave action is smaller for transversal containers (Hinz and Oumeraci 2002, Porraz 1979 and Tekmarine 1982).

2.2.4 Effect of Blocking the Direct Flow through the Gaps

The permeability of a GSC-structure is governed by the gaps between GSCs; therefore, some GSC-structures were built to investigate the reduction of the permeability by overlapping layers of containers transversally (in plan view), thus, blocking the gaps from the first layer. For comparison, the gaps of the first layer of containers were blocked with a second layer of transversal containers (Figure 10).

Figure 10: Effect of Blocking the Direct Flow of the Gaps on the Permeability of GSC-Structures

The model tests results have shown that by blocking the gaps with another container, the permeability of the structure is considerably reduced. This can be clearly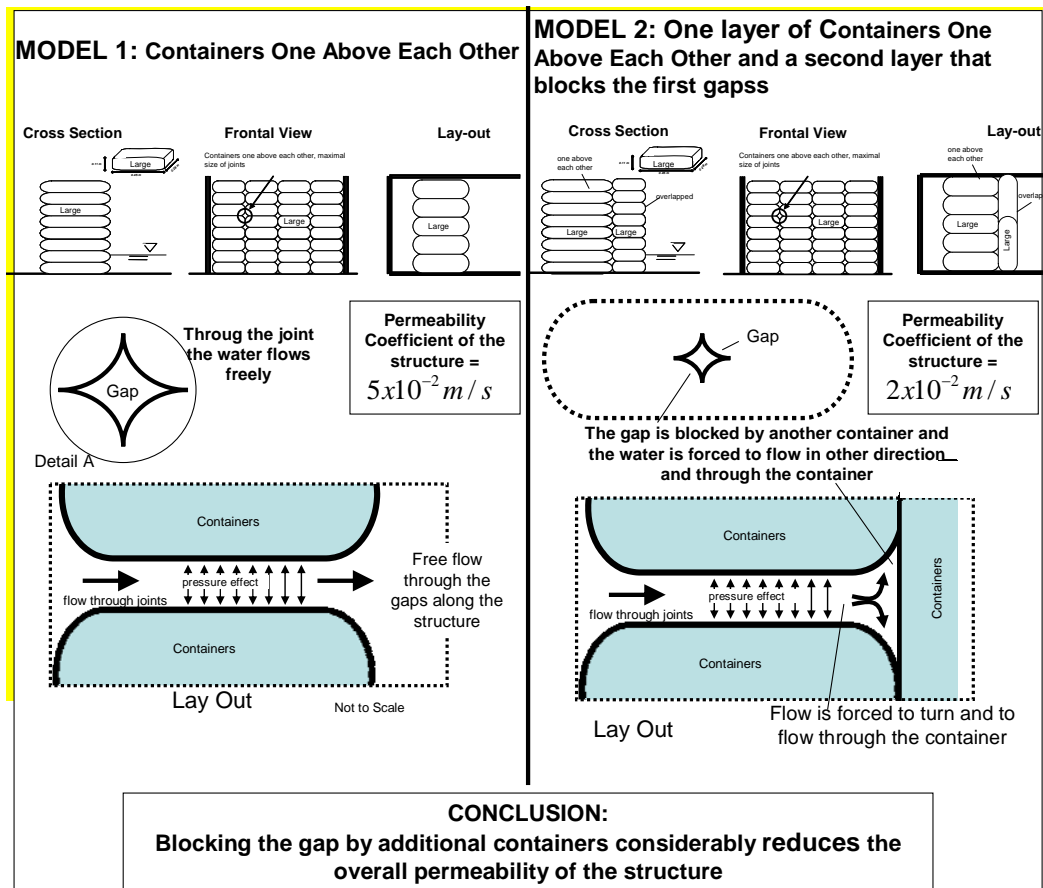 seen in the comparison from Models 1 and 2, where the blocked-structure reduced its permeability considerably (more than twice). This "blocking" is much better achieved with transversal containers, since, the gap is completely blocked (a result that cannot be achieved using two longitudinally placed containers).

This reduction can easily be explained considering that water flows in the first layer through the gaps but when it reaches the second layer, it is forced to flow (at least partially) through the containers and thus, the permeability is reduced (Figure 11).

Therefore, it can be concluded that:
- The permeability of a GSC-structure (and thus the total flow through the structure) is drastically reduced if there is a second layer of overlapped containers that obstruct the flow from the gaps of the first layer (in Lay-out view).
- When a GSC-structure has two or more layers of containers (one transversal and one longitudinal, in plan view), the flow through the structure is too complex and the way the water flow through the structure can hardly be predicted.

Figure 11: Container after the Permeability Tests (marks of water flow clearly seen)

2.2.5 Effect of the Number of Layers on the Permeability

It was seen (section 2.2.2) that two overlapped layers of containers (in plan view) have lower permeability than one layer. Moreover, the influence of a third layer of containers was investigated (Figure 12).

It was concluded from the results that:
- A third layer of containers do not reduce the permeability coefficient of the structure. The total flow will naturally be reduced but the permeability coefficient will remain constant.
- If a GSC-structure has two or more layers of containers then it can be treated as homogeneous structure and further layers will not reduce the permeability coefficient (less flow through the structure due to the increase of its length).
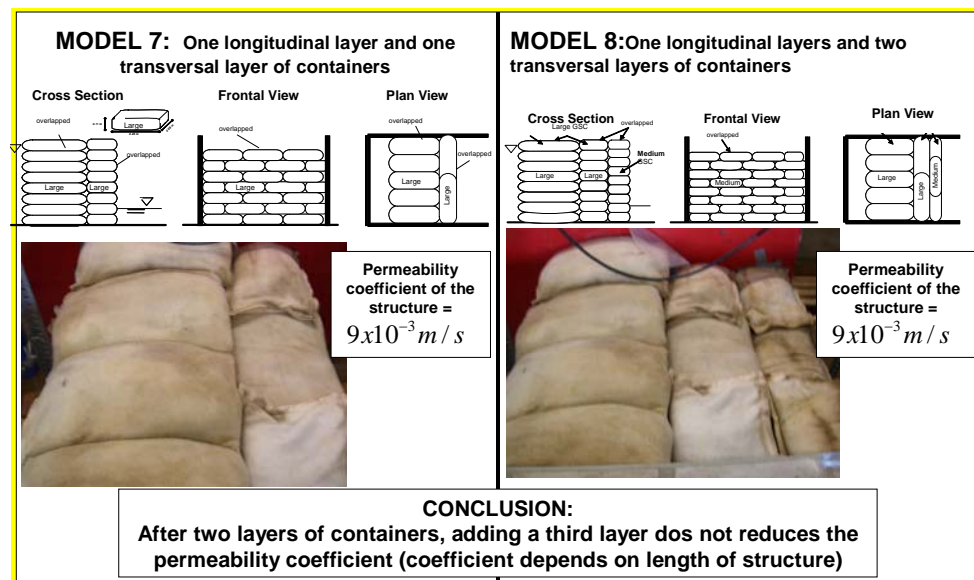- After a second layer, the mode of placement does not have a significant effect on the permeability.

Figure 12: Effect of the Number of Layers of Containers on the Permeability of GSC-Structures

2.2.6 GSC-Structures with Longitudinal Layers of GSC

This analysis is very important because most of the GSC-structures are constructed in two layers (in plan view) of longitudinal containers e. g. Island of Sylt, Germany and Australia in Hinz and Oumeraci (2002) and Restall (2004), respectively.

From the model tests it can be concluded that:
- The total flow through GSC-structures typically used as revetments depends on the size and number of layers of containers.
- The permeability coefficient of these GSC-structures varies from 8 x 10^{-3} m/s (medium containers) to 1.5 x 10^{-2} m/s (large containers).
- Two layers of GSCs have very similar permeability coefficients as one layer of containers when both of the layers are placed longitudinally to the flow. In this case the gaps from the second layer (in Lay-out view) do not obstruct considerably the gaps from the first layer.

Typical GSC-Structures Used as GSC-Revetments

MODEL 6: Containers overlapped

Cross Section   Frontal View   Plan view

MODEL 9: Two longitudinal layers of containers (in Lay-out view)

Cross Section   Frontal View   Plan view

Permeability coefficient of the structure = $1.5x10^{-2} m/s$

Permeability coefficient of the structure = $1.4x10^{-2} m/s$

The permeability coefficient of GSC-structures typically used as revetments depends on the size of GSC, arrangement and length of structure

Figure 13: Permeability Results of Typically GSC-Structures used as Revetments

2.2.7 Summary of the Basic Model Tests

The main results of the analysis may be summarized as follows:

(i) The flow through GSC-structures essentially reduces to the flow through the size of the gaps; i. e. the size of the gap governs the overall permeability of the GSC-structure.

(ii) The smaller the container, the smaller the permeability coefficient of the structure. This can be explained by the size and distribution of the gaps between containers. A structure made with smaller containers will have more and smaller gaps, subsequently the friction losses of the gap flow will be higher.

(iii) If only the permeability performance of the structure is important, then either longitudinally or transversally placed GSCs will provide similar total flows through the structure. However, the hydraulic stability of sand containers under wave action is lower for transversally placed containers than for longitudinally placed GSCs (Oumeraci and Hinz, 2002; Porraz, 1979 and Tekmarine, 1982).

(iv) The permeability of a GSC-structure (and thus the total flow through the structure) is considerably reduced if there is a second layer of overlapped containers that obstructs the flow coming out of the gaps of the first layer (see Figure 4, model 7).

(v) The permeability coefficient of GSC-structures with elements parallel to the flow as commonly used for coastal structures (e. g. Island of Sylt, Germany and Australia in Hinz and Oumeraci 2002 and Restal et al 2004) may vary from 8 x 10^{-3} m/s (medium containers) to 1.5 x 10^{-2} m/s (large containers).

3. Further Permeability Tests and Effect of Permeability on Hydraulic Stability of GSC-Structures

After the permeability tests, further tests on the permeability and its effect on the hydraulic stability of coastal structures such as breakwaters and revetments were performed.

The geometry of the GSC-structure was the same as used in prototype GSC-structures. However, before starting with new tests, the data derived from the model test by Hinz and Oumeraci (2002) performed in the Large Wave Flume at Hannover (GWK) were first analyzed with respect to the permeability of the tested GSC-structure.

3.1 Permeability of GSC-Structure Tested in the Large Wave Flume (GWK)

Model tests were conducted at the large wave flume at Hannover (GWK) in order to investigate the hydraulic stability of GSC-revetments. After the model tests, the time required for the water to flow from behind the structure and the variation of water level before the structure versus time were recorded (Figure 14 and 15). The entire structure consists of a structure made of 150 litre GSCs founded on a sand slope.

The sand slope was covered with a nonwoven geotextile (Figure 14). Since the GSC-structure is placed on a sand slope that is also protecting the coastal area, the permeability was calculated for both GSC-structure and sand slope. For this GSC-structure the derived permeability coefficient is $k = 2x10^{-2}$ m/s (Figure 14).
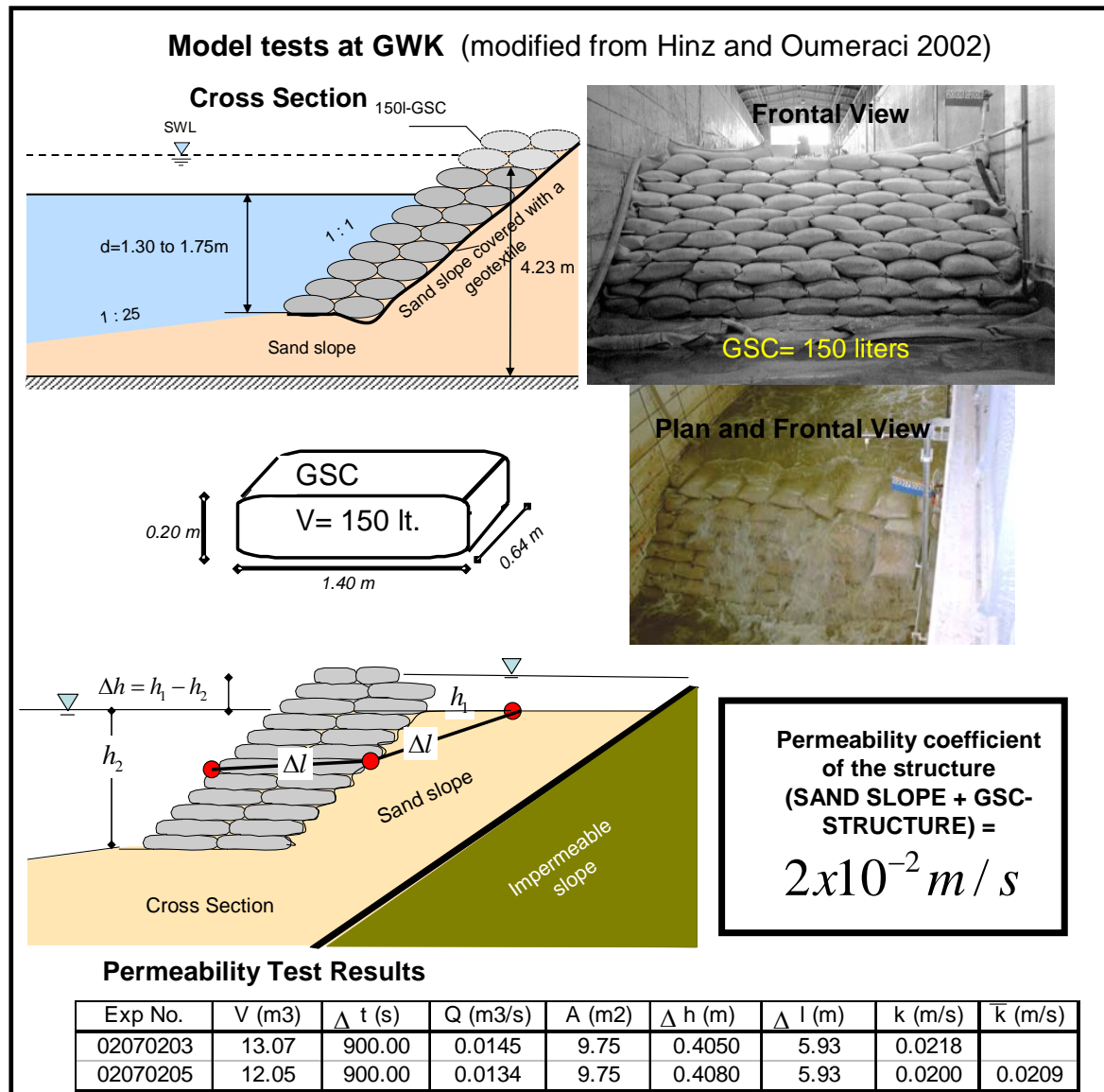
Figure 14: Results of Permeability Tests of a GSC-Revetment in the Large Wave Flume of GWK (modified from Hinz and Oumeraci, 2002)
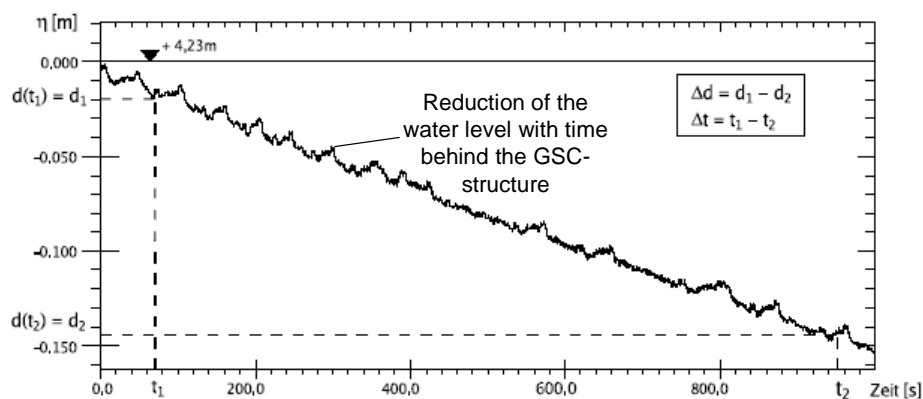

Figure 15: Reduction of Water Level Measured at GWK (average flow obtained indirectly from this graph) (after Hinz and Oumeraci 2002)

3.2 Permeability of GSC-Structures in the Wave-Flume of Leichtweiss-Institute

The model set-up was designed in the same way as in the basic permeability tests (see Figure 1 and Figure 2), with the difference that the tests were performed in the wave flume of LWI (Figure 16).

The revetment was made of large sand containers (0.45m x 0.28m x 0.09m), which were also used in the basic permeability tests (Section 2). The permeability coefficient is around $k=1.4 \times 10^{-2}$ m/s and is almost the same as the coefficient obtained in models 6 and 9 (Table 1).

Permeability of a GSC-Revetment Measured at LWI

$\Delta h = h_1 - h_2$ $i = \dfrac{\Delta h}{\Delta l}$

Three depths were tested: 0.27m, 0.36m, 0.45m

Water was pumped to maintain a zero level behind the structure

$\nabla \quad h_2 = 0$

Permeability coefficient of GSC-structure =

$1.4 x 10^{-2} m/s$

Permeability Test Results

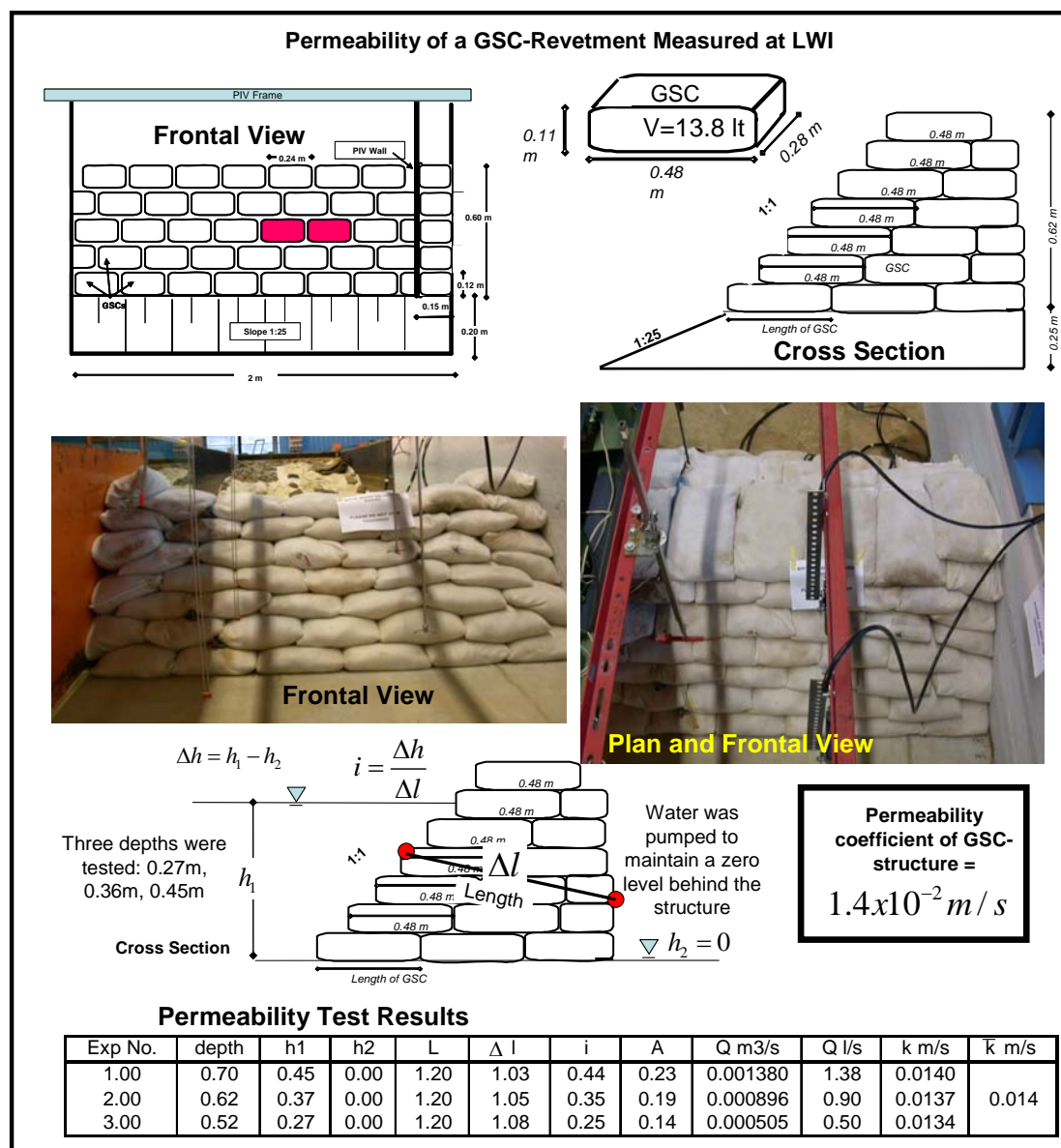| Exp No.	depth	h1	h2	L	Δ l	i	A	Q m3/s	Q l/s	k m/s	k̄ m/s
1.00	0.70	0.45	0.00	1.20	1.03	0.44	0.23	0.001380	1.38	0.0140	
2.00	0.62	0.37	0.00	1.20	1.05	0.35	0.19	0.000896	0.90	0.0137	0.014
3.00	0.52	0.27	0.00	1.20	1.08	0.25	0.14	0.000505	0.50	0.0134	

Figure 16: Results of Permeability Tests of a GSC-Revetment Tested at the Wave-Flume of Leichtweiss Institute (LWI)

3.3 Effect of the Mode of Placement on the Permeability of GSC-Structures
3.3.1 Experimental Set-Up

The configurations tested in the LWI-wave-flume during the second stage of model tests are shown in Figure 17b. A smaller size of containers is used for this purpose (Figure 17a). The primary objective of these tests is to investigate the influence of the mode of placement of GSCs on the permeability of the entire GSC-structure.
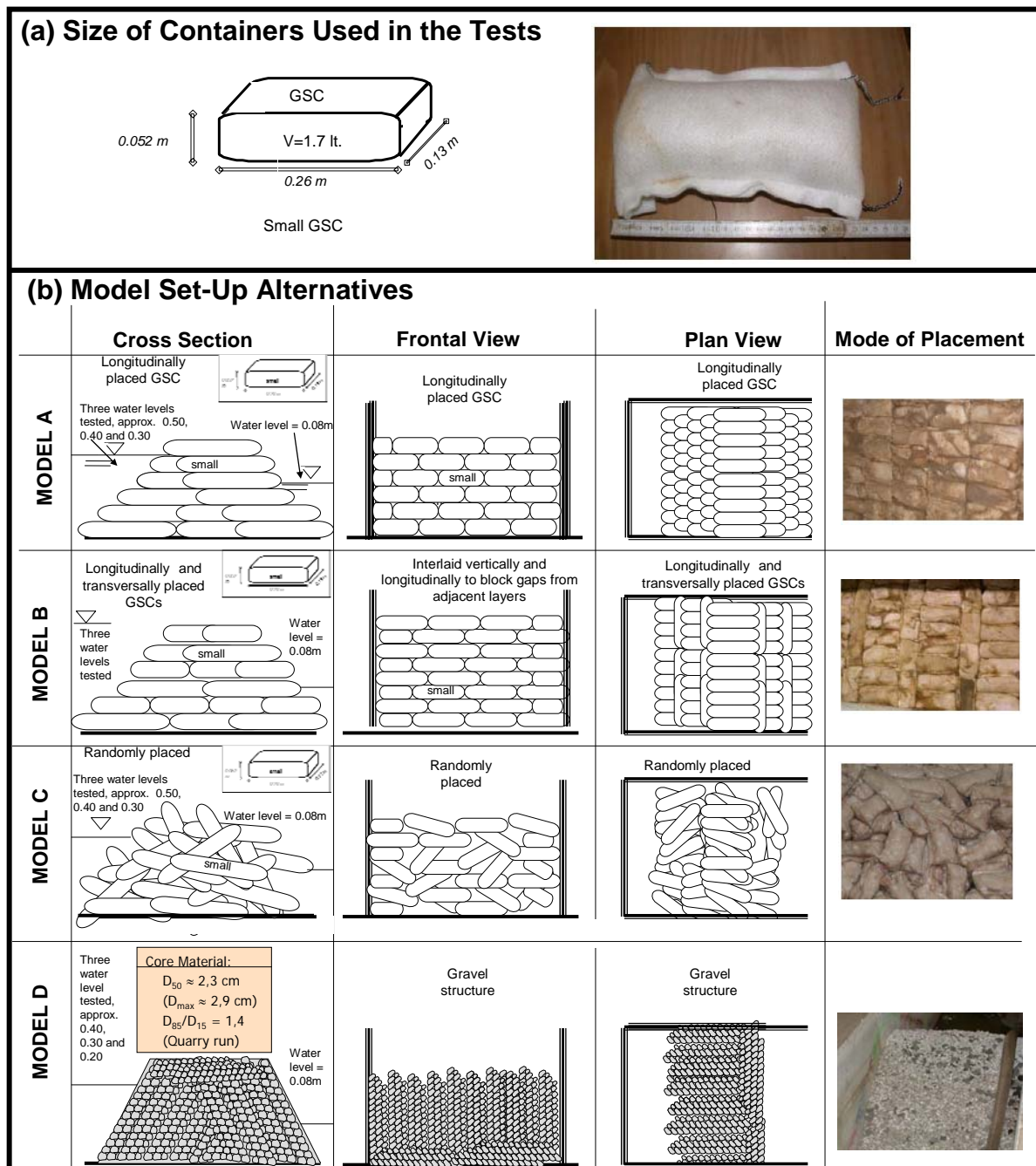

Figure 17: Configurations Tested to Investigate the Effect of the Mode of Placement on the Permeability

Figure 18: GSC-Structure with Randomly Placed Sand Containers

Figure 19: Photos of the Tested Mode of Placement

The structure has a height of approx 0.81 m, and was built with sand containers with the following dimensions: 0.26m length, 0.13m width and 0.052m height (Figure 17a). With this size of container, three types of mode of placement were tested (Figure 17b):

    (i)   **Model A:** GSC-structure with containers placed longitudinally in the wave-flume.

    (ii)   **Model B:** GSC-structure with containers placed both longitudinally and transversally (interlaid) in the wave flume in order to block the gaps of the previous layer.

(iii)   **Model C:** GSC-structure with the containers placed randomly by dropping them from an elevation of about 1m in the wave-flume (Figure 18).

(iv)   **Model D:** A gravel structure with the same geometry as the GSC-structure was also tested for comparison. The gravel structure is made of stones with a diameter of $D_{50} = 2.3$cm, $D_{max}=2.9$cm, $D_{85}/D_{15}=1.4$.

3.3.2 Experimental Results

The results of the permeability tests are summarized in Table 3 and Figure 20. The structure made of randomly placed containers has the highest permeability coefficient of the three tested GSC-structures, because the probability of the water flowing through the structure of finding a "direct" way (with large gap size) across the structure is higher than in the other two configurations. The smallest permeability coefficient is expectedly obtained for the containers placed interlaid in a way that the second layer blocks the gaps of the first layer of containers.

Table 3: Permeability Results of the Second Stage Model Tests

Experiment	wave flume	h1 (m)	h2 (m)	Q m3/s	Δ l	i gradient	Area (m2)	k (m/s)	AVG (m/s)
GEOTEXTILE SAND CONTAINERS RANDOM PLACING									
1.00	2.00	0.36	0.08	0.0016	1.93	0.15	0.44	0.0245	
2.00	2.00	0.36	0.07	0.0016	1.94	0.15	0.43	0.0246	
4.00	2.00	0.36	0.07	0.0022	1.94	0.15	0.42	0.0356	
6.00	2.00	0.50	0.07	0.0026	1.84	0.23	0.57	0.0196	0.02412
7.00	2.00	0.50	0.08	0.0030	1.83	0.23	0.58	0.0226	
8.00	2.00	0.49	0.08	0.0033	1.83	0.22	0.57	0.0261	
9.00	2.00	0.65	0.09	0.0048	1.72	0.33	0.74	0.0201	
10.00	2.00	0.65	0.09	0.0053	1.72	0.33	0.74	0.0219	
11.00	2.00	0.66	0.09	0.0054	1.71	0.33	0.75	0.0221	
GRAVEL CORE									
12.00	1.00	0.35	0.08	0.0131	1.93	0.14	0.22	0.4350	
13.00	1.00	0.35	0.08	0.0123	1.93	0.14	0.22	0.4083	0.38810
14.00	1.00	0.35	0.08	0.0120	1.93	0.14	0.22	0.3987	
15.00	1.00	0.39	0.18	0.0103	1.83	0.12	0.28	0.3104	
GSC Placed BLOCKING GAPS									
22.00	1.00	0.63	0.06	0.0012	1.76	0.33	0.34	0.0110	
23.00	1.00	0.61	0.06	0.0015	1.77	0.31	0.34	0.0141	
24.00	1.00	0.62	0.05	0.0012	1.77	0.32	0.33	0.0109	
25.00	1.00	0.58	0.05	0.0011	1.80	0.30	0.31	0.0117	
26.00	1.00	0.68	0.06	0.0016	1.73	0.36	0.37	0.0123	0.01244
27.00	1.00	0.66	0.06	0.0018	1.74	0.35	0.36	0.0145	
28.00	1.00	0.65	0.10	0.0016	1.71	0.32	0.37	0.0130	
29.00	1.00	0.50	0.04	0.0007	1.86	0.25	0.27	0.0110	
30.00	1.00	0.48	0.04	0.0007	1.87	0.23	0.26	0.0107	
31.00	1.00	0.48	0.05	0.0009	1.87	0.23	0.26	0.0152	
GSC Placed LONGITUDINALLY									
30.00	1.00	0.36	0.05	0.0007	1.95	0.16	0.21	0.0228	
31.00	1.00	0.35	0.04	0.0006	1.96	0.16	0.20	0.0201	
33.00	1.00	0.35	0.05	0.0009	1.96	0.15	0.20	0.0291	
34.00	1.00	0.50	0.05	0.0010	1.85	0.24	0.28	0.0148	
36.00	1.00	0.49	0.05	0.0020	1.86	0.24	0.27	0.0310	0.02274
37.00	1.00	0.49	0.06	0.0020	1.85	0.23	0.28	0.0310	
38.00	1.00	0.65	0.06	0.0024	1.75	0.34	0.35	0.0196	
39.00	1.00	0.64	0.05	0.0022	1.76	0.34	0.35	0.0192	
40.00	1.00	0.64	0.06	0.0020	1.75	0.33	0.35	0.0171	

Further interesting results is the comparison among the obtained permeability coefficients: the permeability of the sand material ($k=10^{-3}$) is approximately ten times smaller than the permeability of the GSC-structure ($k=10^{-2}$); moreover, the permeability of the GSC-structure ($k=10^{-2}$) is approximately ten times smaller than the coefficient of a gravel structure ($k=10^{-1}$).

Finally, randomly placed sand containers and longitudinally placed containers have similar permeability (randomly placed slightly higher than longitudinally). This can be explained because in the longitudinal containers, the water-flow has a direct way across the structure through the longitudinal gaps. However, these gaps are smaller than the gaps that appear between randomly placed containers.

Model Structure	Description	Darcy's Permeability Coefficient k (m/s)
	Structure made of geotextile sand containers placed interlaid blocking the gaps of the previous layer	1.244×10^{-2}
	Structure made of geotextile sand containers placed longitudinally to the flow	2.274×10^{-2}
	Structure made of geotextile sand containers placed randomly	2.412×10^{-2}
	Structure made of gravel (D_{50} = 2.3 cm, D_{max}=2.9cm, D_{85}/D_{15}=1.4).	3.881×10^{-1}

Remark: Permeability of gravel is normally higher than 10^{-2}m/s and permeability of sand is between 1×10^{-3} and 3×10^{-3}m/s.

Figure 20: Comparison of Permeability Coefficients with Different Mode of Placement

4. Effect of Permeability on the Hydraulic Stability of GSC-Structures

The mode of placement may significantly affect the permeability of a GSC-structure. In the wave-flume of LWI, the same GSC-structures as in section 3 (small containers with same geometry and same size but with different mode of placement and thus different permeability) are tested under wave action to investigate the influence of the permeability and mode of placement on the hydraulic stability.

In the wave-flume, each of the three configurations as shown in Figure 20 were subject to increasing regular wave heights until the structure collapsed. The wave period was maintained constant (T=2s). Thus, if one structure resisted 100 regular waves of a specific wave height, wave generation will stop, and after 20 minutes the structure was subject to wave action with another series of higher 100 waves. In the

same way, the wave height was increased until the structure collapsed. After collapse, the structure was rebuilt and the experiment with the same wave height was repeated for verification.

Mode of Placement of GSCs	Wave Height (H) (m)	Wave Period (T) (sec)	Water Depth (d) (m)	Hydraulic Stability	GSCs Displaced after Wave Action
Longitudinal	H = 0.08	T = 2	d =0.50	Stable	0
	H = 0.12	T = 2	d =0.50	Stable	0
	H = 0.16	T = 2	d =0.50	Stable	0
	H = 0.20	T = 2	d =0.50	Stable	0
	H = 0.24	T = 2	d =0.50	UNSTABLE	9
Interlaid	H = 0.08	T = 2	d =0.50	Stable	0
	H = 0.12	T = 2	d =0.50	Stable	0
	H = 0.16	T = 2	d =0.50	UNSTABLE	38
Random	H = 0.08	T = 2	d =0.50	Stable	0
	H = 0.12	T = 2	d =0.50	Stable	0
	H = 0.16	T = 2	d =0.50	UNSTABLE	23

Figure 21: Effect of Permeability and Mode of Placement on the Stability of GSC-Structures

The results of the model tests of structures with different mode of placement under wave action are shown in Figure 21. As expected, the structure with the lower permeability showed the lower resistance against wave action. The higher permeability behind the first layer dissipates the pressures behind the structure, thus, providing higher hydraulic stability.

The comparison between containers placed randomly and longitudinally shows that the latter have a higher stability than the randomly placed containers. This is obvious, since only surface piercing structures were tested. Therefore, the displacements started at the slope where the contact areas and the contribution of the weight of neighbouring containers contribute to the hydraulic stability of the GSCs (Figure 22).

This result on the higher stability of longitudinal containers applies only for surface piercing structures, since Grüne et al (2006), showed that with submerged structures made of GSCs, the critical container is the one placed at the crown of the structure (which has reduced contact areas and no weight contribution from neighbouring containers).
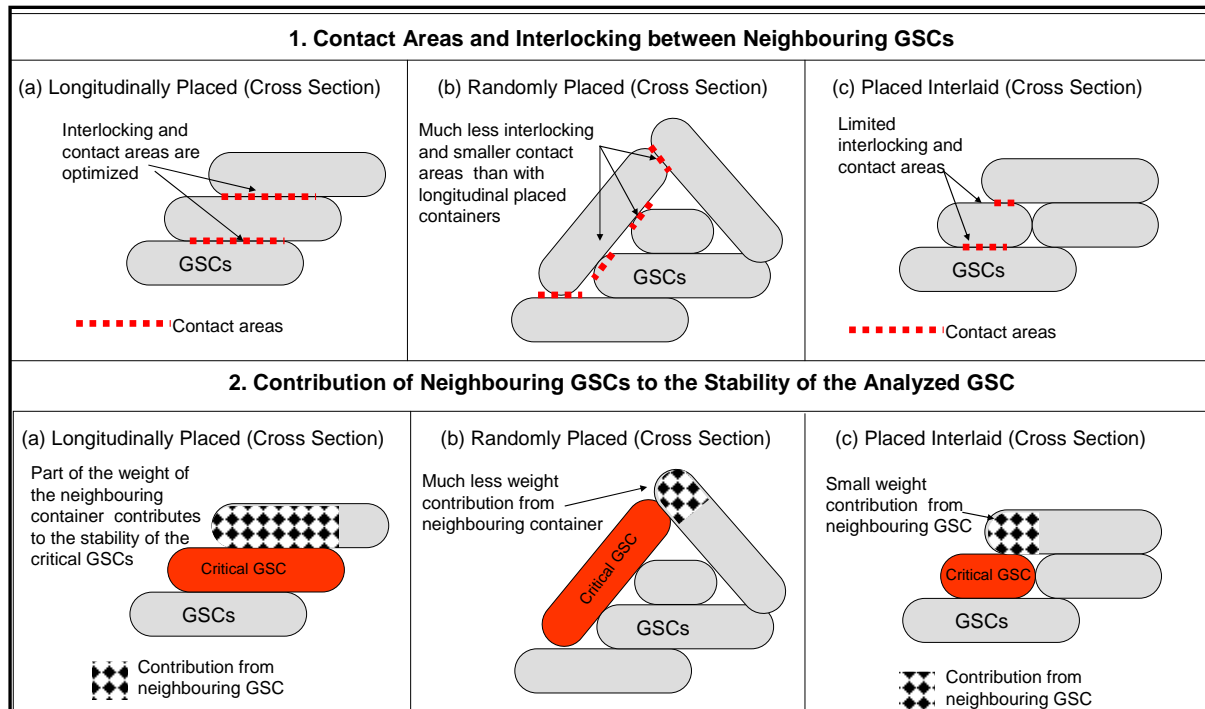
Figure 22: Comparison of Contact Areas and Contribution of Neighbouring GSCs on the Hydraulic Stability between Tested GSC-Structures

5 Failure Mechanisms of a Coastal Structure Made of GSCs Placed Randomly

Recio and Oumeraci (2005) and (2006) and Hinz and Oumeraci (2002) clarified the types of displacement and failure mechanisms of several GSC-structures with regularly placed containers (longitudinally), however, up to date no information on the failure mechanisms of a structure with the containers placed randomly is available. Therefore, using the video documentation, the failure mechanisms of a GSC-structure with the containers placed randomly was clarified. Figure 23 shows in three phases, the failure mechanisms of a surface piercing GSC-structure with containers placed randomly.

The failure mechanisms of a GSC-structure with randomly placed containers may be summarized as follows:
   a) The containers that are on the slope and are not overlapped with other containers will be the first to move, these containers will simply slide to the toe of the structure during down rush (Figure 23a).
   b) The displacement of the first containers will "expose" other containers, or will reduce the interlocking of other containers. Thus, the containers that have been "exposed" by previous displacements of containers will be displaced during down rush of the next wave cycles (figure 23 b).
   c) The collapse process will continue; each container that is displaced reduces the contact areas and interlocking of other containers, which in the next waves will be displaced (figure 24 c).
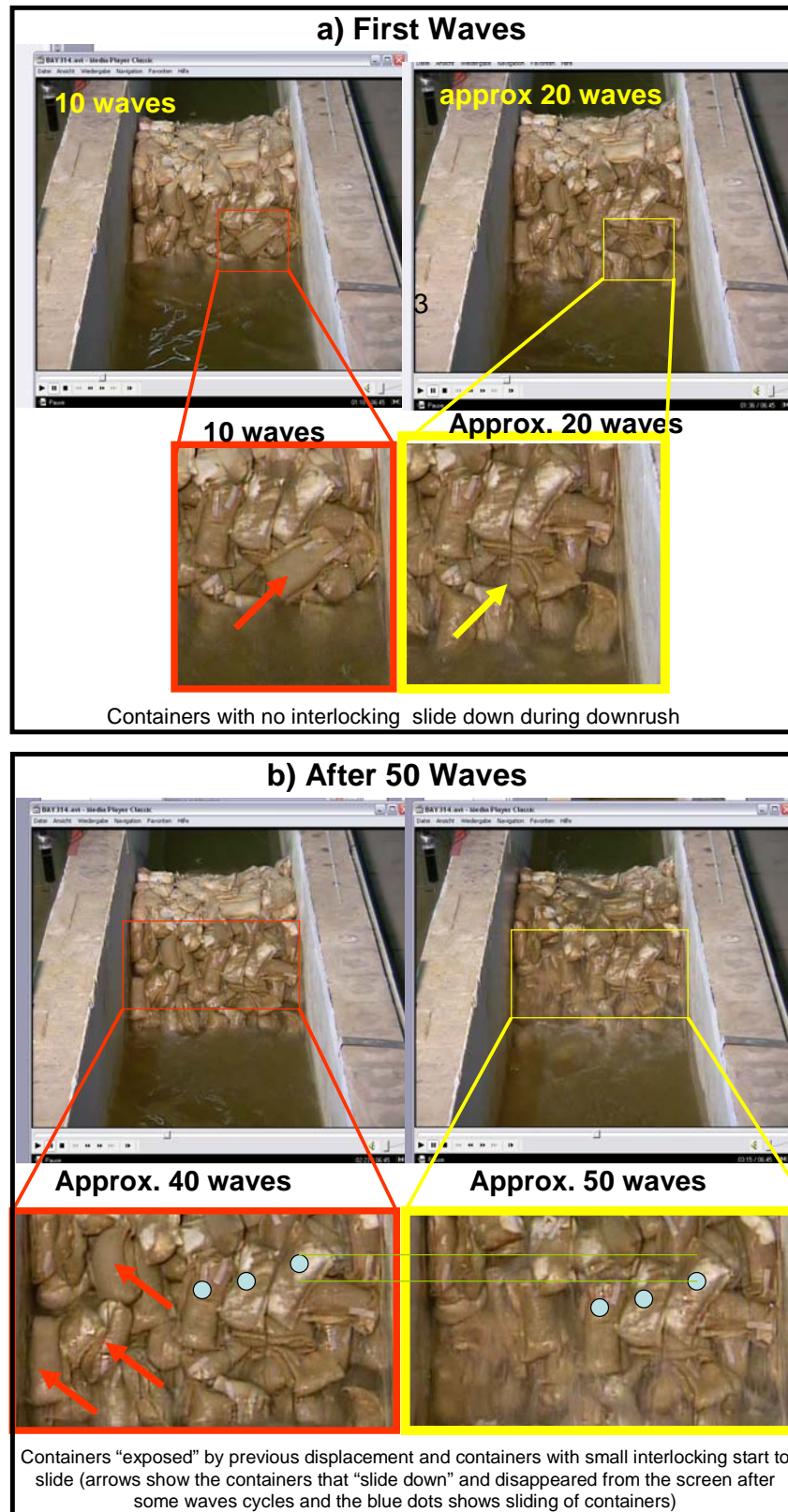
Figure 23: Failure Mechanisms of a GSC-Structure with the Containers Placed Randomly (continues on next page)
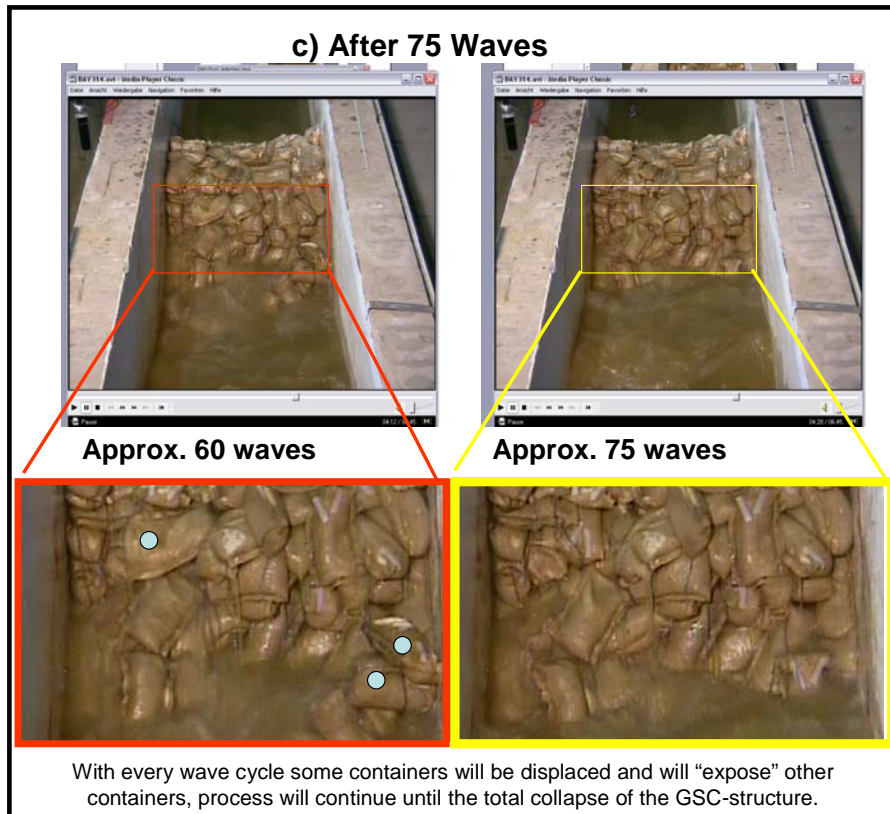
Figure 23: Failure Mechanisms of a GSC-structure with the Containers Placed Randomly

6. Overall Summary of Permeability Tests
The most important results obtained from all permeability tests described in section 2 to 5 are summarized in Figure 24, showing that:

a) The permeability of a GSC-structure depends mainly on the size of the gaps. The flow through a GSC-structure is governed by flow through the gaps and thus, the flow through the sand container can be neglected.

b) If no reliable data are available, a permeability coefficient for GSC-structures of $k = 10^{-2}$ m/s would be reasonable.

c) The optimal arrangement to reduce the permeability of a GSC-structure is by blocking the gaps of the fist layer with transversal containers of a second layer (see models 7 and 11 in Figure 4 and Table 1). With this mode of placement the permeability coefficient is approximately 5×10^{-3} m/s.

d) The mode of placement of the sand containers in a GSC-structure considerably affects the permeability of the structure. Random placing has the highest permeability, but smaller hydraulic stability for surface piercing structures than longitudinally placed containers.
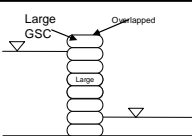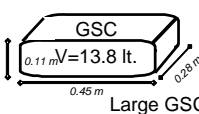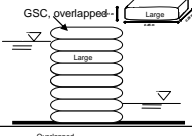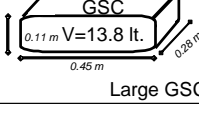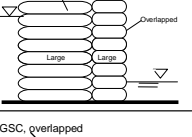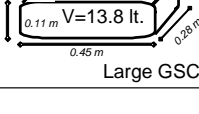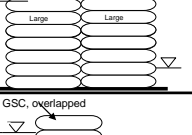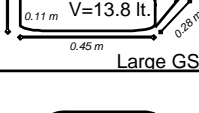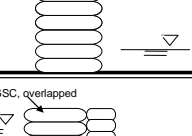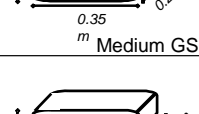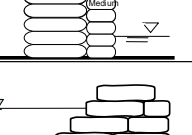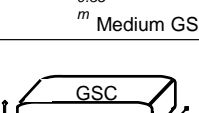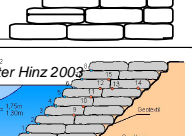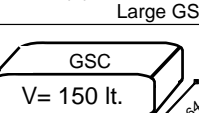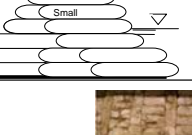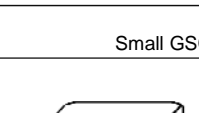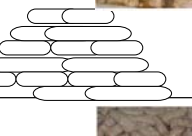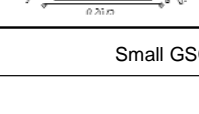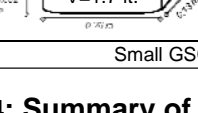
	Cross Section	Size GSC	Permeability k (m/s)	Remarks
MODEL 5		GSC, V=13.8 lt., 0.11 m, 0.28 m, 0.45 m, Large GSC	$8x10^{-3}$	-Transversal GSC-structures have smaller permeability.
MODEL 6		GSC, V=13.8 lt., 0.11 m, 0.28 m, 0.45 m, Large GSC	$1.5x10^{-2}$	- One typical structure used for GSC-revetments.
MODEL 7		GSC, V=13.8 lt., 0.11 m, 0.28 m, 0.45 m, Large GSC	$9x10^{-3}$	- Optimal structure if minimal permeability is needed.
MODEL 9		GSC, V=13.8 lt., 0.11 m, 0.28 m, 0.45 m, Large GSC	$1.4x10^{-2}$	- Most typical structure used as GSC-revetment.
MODEL 10		V= 7.5 lt., 0.09, 0.24 m, 0.35 m, Medium GSC	$8x10^{-3}$	-Small containers induce lower permeability.
MODEL 11		V= 7.5 lt., 0.09, 0.24 m, 0.35 m, Medium GSC	$7x10^{-3}$	-Blocking directly the gaps reduces considerably the permeability.
LWI		GSC, V=13.8 lt., 0.11 m, 0.28 m, 0.45 m, Large GSC	$1.4x10^{-2}$	- GSC-revetments built only with sand containers.
GWK	After Hinz 2003	GSC, V= 150 lt., 0.64 m, 1.40 m, GWK-GSC	$2x10^{-2}$	- This permeability coefficient is for a GSC-structure with a sand slope. Based on data from Hinz and Oumeraci (2002).
MODEL A		V=1.7 lt., 0.050 m, 0.53 m, 0.20 m, Small GSC	$2.2x10^{-2}$	-Small containers placed longitudinally, higher hydraulic stability than randomly placed for surface piercing structures.
MODEL B		V=1.7 lt., 0.050 m, 0.53 m, 0.20 m, Small GSC	$1.2x10^{-2}$	-Small containers placed longitudinally and transversally, each layer blocking the gaps from previous layer. Lowest stability.
MODEL C		V=1.7 lt., 0.050 m, 0.53 m, 0.20 m, Small GSC	$2.4x10^{-2}$	- Small containers placed randomly, higher permeability but smaller stability compare with longitudinal containers.

Figure 24: Summary of Results

7. Conceptual Model for the Permeability of GSC-Structures

The permeability of GSC-structures has shown to be governed by the gaps between sand containers. Based on this conclusion a conceptual model including the size and shape of the gaps is first proposed. Recommendations are then provided to derive the permeability of GSC-structures based on simple parameters such as the dimensions of the container.

Several researchers have tried with mixed results to obtain a discharge formula through porous structures as a function of parameters such as hydraulic gradient, porosity, grain size, and geometry of the structure.

Soil-Mechanics textbooks (i.e. Vafai 2000) give general approaches for deriving the permeability of porous structures (already explained in section 1). For gravel and coarser soils, Scheidegger 1974 and Aberg 1992 proposed complex expressions, which consider the inertia force on the gravel to describe the permeability. Sawaragi 1992 found that for coarser porous structures, the permeability and the turbulent drag coefficient in the Forcheimer type equation in the unsteady flow are different from those in the steady flow. Williams 1992 modified the Forcheimer equation, deriving the empirical coefficients α and β considering the average roughness of the grains (see section 1 for details on the coefficients).

For coastal structures, several researchers have implemented the Forcheimer equation to simulate wave induced action through a porous media (i.e. van Gent 1995, Liu 1999 and 2005).

Finally, Michioku 2005 investigated the discharge through a permeable structure and formulated the flow discharge through the porous structure as a function of hydraulic gradient, porosity and grain size.

The peculiarity of a GSC-structure is that it has well defined gaps, which govern the flow through the structure.

Previous studies have shown that to date, there is no conceptual model that can be applied directly to the permeability of GSC-structures. The peculiarities of a GSC-structure are, that it has: (i) inhomogeneous materials (GSCs consist of sand and geotextile) and (ii) well defined gaps between GSCs, which govern the flow through the structure.

For the conceptual model presented in this study a simplified model based on energy conservation is presented.

7.1 Assumptions

The following assumptions (Figure 25) are made to derive the conceptual model:

i. The flow through the sand container itself is neglected (impermeable GSCs), so that the permeability of the structure is solely determined by the flow through the gaps.

ii. The gaps among neighbouring containers are considered as triangular pipes which may then be transformed to a hydraulically equivalent diameter.

iii. The Reynolds number of the gap flow is directly related to the size of the gaps.

iv. The size of the gaps is considered constant (in reality, the size of the gaps varies slightly depending on their location in the structure).

v. Flow resistance along the gap (water-geotextile-interface) is constant.

vi. Flow velocities upstream of the structure can be neglected ($v_\infty = 0$). Flow in gaps is only induced by difference of water levels in front and behind the structure.

vii. Only the friction losses along the gap (triangular pipe) are considered, inflow and outflow losses are neglected.
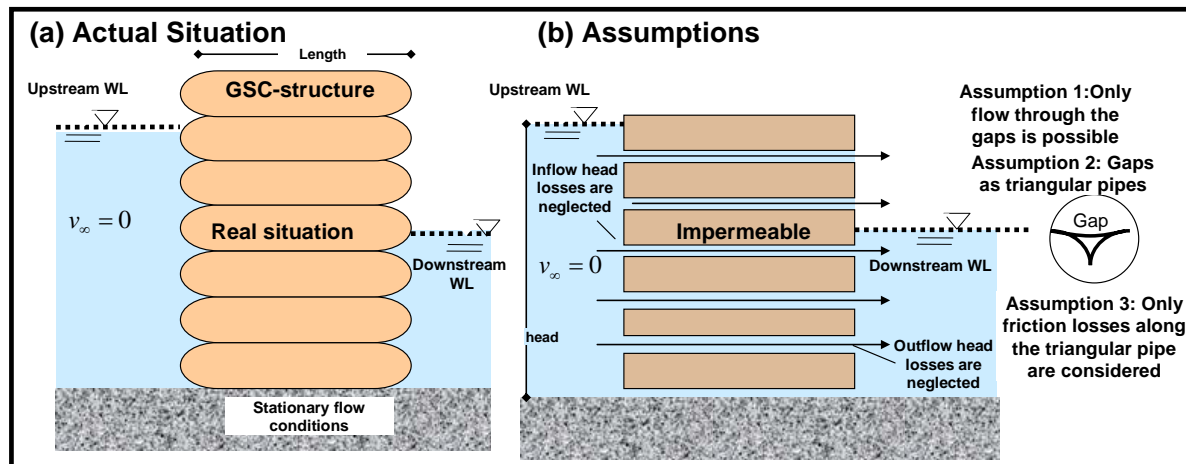
Figure 25: Assumptions of This Analysis

7.2 Conceptual Model

Moreover, the GSC-structure is considered two dimensional and divided in three regions (Figure 26c) in which energy conservation is maintained:

Zone A: Interface between the upstream flow and the GSC-structure (Figure 26c):

The interface between structure and upstream flow where the latter suddenly converges from the open flow to the triangular pipe (gap along the GSC-structure).

The initial velocities at the entrance of each gap of the structure are obtained by assuming that the flow transition is analogous to a sudden pipe contraction, thus, the velocity at the entrance of the gap is induced by the hydraulic gradient at the gap minus the local losses induced by the contraction.

Zone B: Flow through the structure along each of the individual gaps:

Zone B compromises the length of the flow channel from the beginning of the gap to the end of the gap (Figure 26c). In this zone, the velocity at the beginning of the gap is equal to the velocity at the end of the gap minus friction losses due to the roughness along the gap.

Zone C: Interface between the structure and the downstream flow:

The interface between the end of the gap and the downstream flow where the flow diverges from the triangular gap-pipe to the open flow downstream (Figure 26c). The interface between the GSC-structure and the downstream flow is treated as a simple

wave discharge problem where the velocity after the end of the gap is equal as the velocity at the beginning of the gap plus losses.
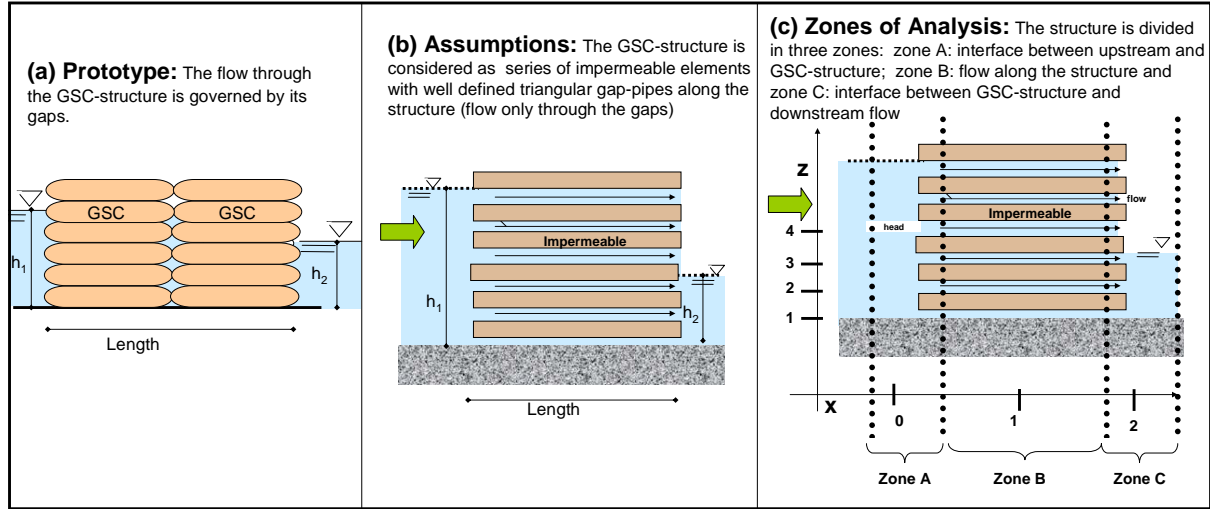

Figure 26: Principle of the Conceptual Model

Thus, considering the afore-mentioned zones, the flow through the gap can be described as:

$$\frac{v_0^2}{2g} + \frac{p_0}{\rho_w g} + z_0 - h_0 = \frac{v_1^2}{2g} + \frac{p_1}{\rho_w g} + z_1 - h_r = \frac{v_2^2}{2g} + \frac{p_2}{\rho_w g} + z_2 - h_0 = const. \qquad (6)$$

where v_i is the velocity at point i (Figure 26c), p_i is the pressure at point i, ρ_w is the density of water, h_r is the friction head losses along the gap, h_0 is the inflow and outflow head losses, g is gravity acceleration and z_i (Figure 26c) is the height of the measurement point in the direction of gravity.

Recalling the assumptions of the study, where the local losses are neglected, then, equation 6 can be re-written as follows:

$$\frac{v_0^2}{2g} + \frac{p_0}{\rho_w g} + z_0 = \frac{v_1^2}{2g} + \frac{p_1}{\rho_w g} + z_1 - h_r = \frac{v_2^2}{2g} + \frac{p_2}{\rho_w g} + z_2 = const. \qquad (7)$$

where h_r can be defined as:

$$h_r = \lambda \frac{L}{D_{eq}} \frac{v^2}{2g} \qquad (8)$$

where L is the length of the gap, D_{eq} is the equivalent diameter of the gap-pipe, v is the velocity in the gap, g is the gravity acceleration and h_r is the friction head loss.

The friction factor λ is a function of the Reynolds number Re and influenced by the relative roughness of the pipe k_{fric} / D_{eq}, where k_{fric} is the roughness of the material used in the pipe (in this case, the roughness of the geotextile). The roughness of each material is determined experimentally. Reynolds number can be defined as:

$$\mathrm{Re} = \frac{v D_{eq}}{v} \qquad (9)$$

where v is the velocity in the pipe, v is the kinematic viscosity of water and D_{eq} is the equivalent diameter of the pipe. For a triangular pipe, like the gaps in a GSC-structure, D_{eq} can be defined as:

$$D_{eq} = 4R_h \qquad (10)$$

where the hydraulic radius R_h can be defined as:

$$R_h = \frac{A}{P} \qquad (11)$$

where A is the cross area and P is the wet perimeter of the pipe.

7.3 Pipe Friction Factor of GSC-Gaps

Equation 7 describes the flow of each gap in the GSC-structure. The total flow through the structure is obtained by summing up the flow through individual gaps. However, to solve equation 7, the friction factor λ needs to be accurately determined as a function of the flow regime:

(i) For laminar flows, Poiseuille's equation is applied (Re<2320):

$$\lambda = \frac{64}{\mathrm{Re}} \qquad (12)$$

(ii) For turbulent flow three equations are proposed, depending on how developed the turbulent flow is (Oumeraci 1999):

For hydraulic smooth regime $\left(\mathrm{Re} \dfrac{k_{fric}}{D_{eq}} < 65 \right)$:

$$\lambda \approx \frac{0.309}{(\lg \mathrm{Re} - 0.845)^2} \qquad (13)$$

For the transition regime ($65 < \mathrm{Re} \dfrac{k_{fric}}{D_{eq}} < 1300$):

$$\frac{1}{\sqrt{\lambda}} = 2.0 \cdot \lg \left(\frac{2.51}{\mathrm{Re}\sqrt{\lambda}} + \frac{k_{fric}/D_{eq}}{3.71} \right) \qquad (14)$$

and for fully turbulent flow ($\mathrm{Re} \dfrac{k_{fric}}{D_{eq}} > 1300$):

$$\lambda \approx \left(\dfrac{1}{2 \cdot \lg\left(\dfrac{3.71}{k_{fric} / D_{eq}} \right)} \right)^2 \qquad\qquad\qquad (15)$$

The only unknown for determining the flow through each gap in a GSC-structure and thus, through the whole GSC-structure is the pipe friction factor λ, which for turbulent flows requires the knowledge of the roughness of the gap-pipe k_{fric} (roughness of geotextile).

The roughness k_{fric} can be derived from the data obtained from the basic permeability tests (section 1). In this way, the roughness k_{fric} of the gap-pipe will implicitly account for other effects that are not considered in the conceptual model such as variations of the pipe-gap, flow through the containers itself, etc.

Using the permeability test results, the relative-roughness of GSC-gaps k_{fric}/D_{eq} and thus, the pipe friction factor λ are determined iteratively (Figure 27 and Table 4). For turbulent flows, the relative roughness of GSC-gaps is found to be around $k_{fric}=$ 0.6mm. The value is plausible, if compared with the values of known materials.
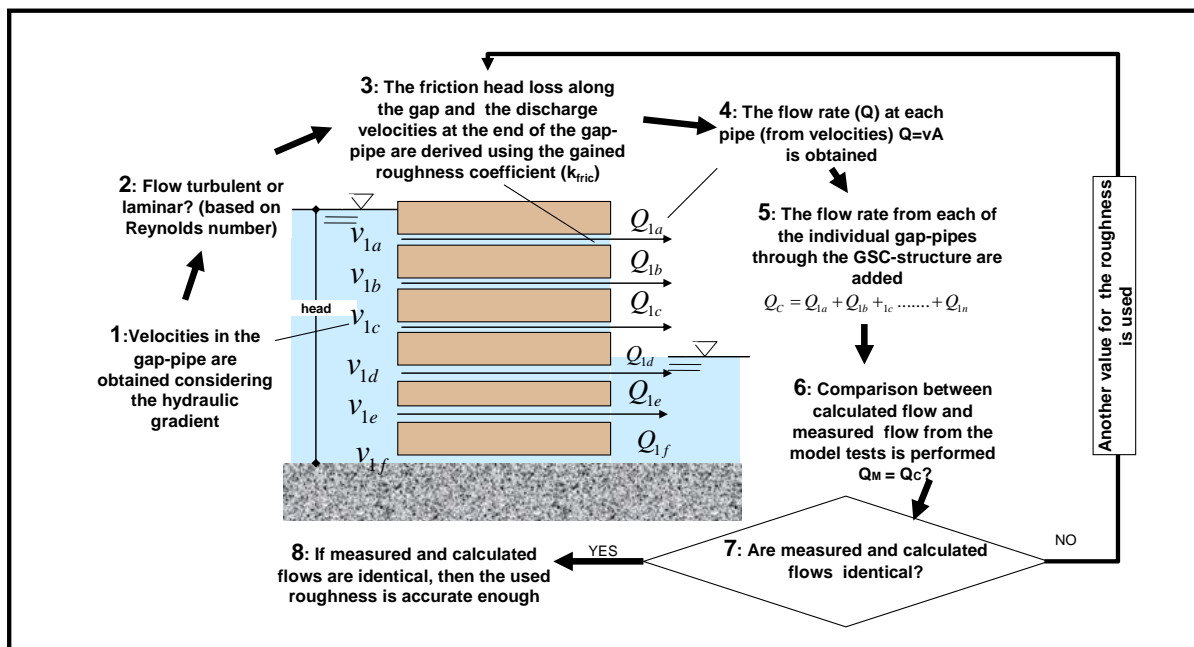

Figure 27: Iterative Procedure to Determine the Roughness k_{fric} of Gap-Pipes in GSC-Structures

Table 4: Results for Obtaining the Friction Factors (with k_{fric}=0.0006m)

Input Values (in meters)	
base joint	0.025
height joint	0.013
area jonint	1.56E-04
perimeter joint	0.081
gravity	9.810
viscocity water	1.00E-06
hydraulic diameter	0.008

Hydralic head m	Vel at begining pipe v m/s	Reynolds number	turbulent?	friction factor	friction head loss	Vel end of pipe	flow at analyzed joint	Q x number of joints at same level Q=va*9	Total flow of Strucutre Qtotal
0.080	1.253	9678.696	yes	0.016	0.077	0.247	0.00004	0.00035	
0.180	1.879	14518.045	yes	0.016	0.173	0.371	0.00006	0.00052	
0.280	2.344	18107.183	yes	0.016	0.269	0.462	0.00007	0.00065	0.003
0.380	2.730	21094.230	yes	0.017	0.365	0.538	0.00008	0.00076	
0.380	2.730	21094.230	yes	0.017	0.365	0.538	0.00008	0.00076	

It was found that for turbulent flows, the relative roughness of GSC-gaps is around k_{fric}= 0.6mm. the value is plausible if we compare it with the values of Table 1 of Annex 2. This roughness is equivalent to the roughness of wood. In reality the roughness of the geotextile is higher than the roughness of wood. However, if we consider that this study assumes the geotextile sand containers as impermeable which in reality they are not (very small flow through them is expected). This roughness value k_{fric} covers slightly the flow through the containers itself.
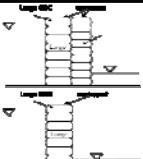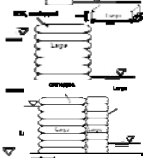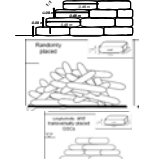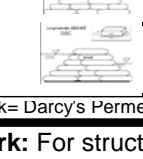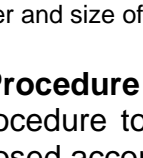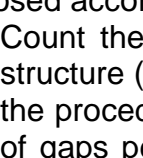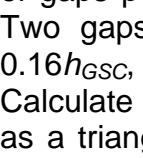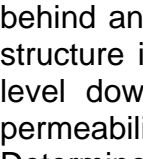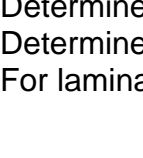
Thus, the roughness of the gaps-pipes for GSC-structures when using the approach presented here is, **k_{fric}=0.6mm**

7.4 Validation of the Conceptual Model

To validate the proposed conceptual model and the derived roughness k_{fric} for GSC-pipe-gaps, the results of the permeability tests of sections 2 and 3 are compared with calculated results obtained by using the conceptual model (Table 5).

The difference between calculated and measured results depends on the type of structure being compared: (i) for longitudinal placed containers, measured and calculated results vary from 1% to 48%; (ii) for interlaid containers from 0% to 33%; (iii) for GSC-structures the variation depend on the size of the container. For large containers, the agreement is within 32%. Moreover, for small containers (randomly and longitudinal placed GSCs) the agreement is not good, however, results are always in the same order of magnitude. The reason for the large disagreement between measured and calculated results for small containers might be due to the very small size of the gaps between small containers (less than 1cm). With such a small gap-size, the difference of flow velocities along the gap and velocity through the container itself are not so large. Therefore, the assumption that the flow is governed only by the gaps is no longer valid.

Table 5: Validation of the Obtained Coefficients (see also Table 2)

Nr.	Structure	Test No.	Model Model	h1 (m)	h2 (m)	MEASURED k m/s	MEASURED k AVG	CALCULATED k m/s	CALCULATED k AVG	Mes/Cal	Mes/Cal AVG
4		4a	4	0.52	0.11	0.0056		0.0068		0.820	
		4b	4	0.47	0.11	0.0064	0.005	0.0064	0.007	1.005	0.769
		4c	4	0.40	0.11	0.0055		0.0063		0.873	
		4d	4	0.54	0.11	0.0058		0.0061		0.949	
5		5a	5	0.52	0.11	0.0081		0.0052		1.560	
		5b	5	0.46	0.11	0.0081	0.008	0.0048	0.005	1.693	1.529
		5c	5	0.39	0.11	0.0079		0.0057		1.386	
6		6a	6	0.43	0.11	0.0163		0.0143		1.137	
		6b	6	0.52	0.11	0.0144	0.015	0.0146	0.014	0.983	1.059
		6c	6	0.47	0.11	0.0138		0.0136		1.017	
7		7a	7	0.55	0.11	0.0096		0.0081		1.185	
		7b	7	0.42	0.11	0.0096	0.009	0.0101	0.009	0.953	1.000
		7c	7	0.48	0.11	0.0150		0.0088		1.705	
8		8a	8	0.46	0.11	0.0107		0.0071		1.512	
		8b	8	0.43	0.11	0.0103	0.010	0.0085	0.008	1.210	1.333
		8c	8	0.48	0.11	0.0094		0.0069		1.362	
9		9a	9	0.48	0.11	0.0153		0.0193		0.794	
		9b	9	0.42	0.11	0.0147	0.014	0.0196	0.020	0.748	0.718
		9c	9	0.45	0.11	0.0142		0.0196		0.724	
10		10a	10	0.47	0.11	0.0082		0.0045		1.823	
		10b	10	0.39	0.11	0.0082	0.008	0.0053	0.005	1.554	1.633
		10c	10	0.52	0.11	0.0082		0.0049		1.673	
11		11a	11	0.51	0.11	0.0073		0.0079		0.923	
		11b	11	0.48	0.11	0.0072	0.007	0.0070	0.007	1.024	0.938
		11c	11	0.44	0.11	0.0074		0.0075		0.984	
GSC		GSC1	gsc	0.45	0.00	0.0140		0.0198		0.707	
		GSC2	gsc	0.36	0.00	0.0137	0.014	0.0200	0.020	0.685	0.687
		GSC3	gsc	0.27	0.00	0.0134		0.0200		0.670	
Ran		Random1	ran	0.36	0.08	0.0245		0.0788		0.311	
		Random2	ran	0.50	0.08	0.0266	0.024	0.0788	0.079	0.338	0.309
		Random3	ran	0.65	0.70	0.0219		0.0788		0.278	
Int		Interlaid1	inter	0.63	0.06	0.0110		0.0450		0.244	
		Interlaid2	inter	0.68	0.06	0.0123	0.011	0.0480	0.047	0.256	0.243
		Interlaid3	inter	0.50	0.05	0.0110		0.0480		0.229	
Lon		Longitu1	lon	0.50	0.05	0.0148		0.0788		0.188	
		Longitu2	lon	0.64	0.05	0.0192	0.019	0.0788	0.079	0.244	0.240
		Longitu3	lon	0.36	0.05	0.0228		0.0788		0.289	

k= Darcy's Permeability Coeff; Measured = Permability Tests; Calculated= Conceptual Model; AVG=average

Remark: For structures made of interlaid GSCs (i. e. models 7, 8, 11), the conceptual model considered the number and size of gaps of the smallest layer (in plan-view)

7.5 Procedure for the Assessment of the Permeability of GSC-Structures

A procedure to determine the Darcy's permeability coefficient of GSC-structures is proposed according to the following steps (Figure 28):

i. Count the number of gaps, measure its size and measure its position in the structure (hydraulic head on each of the gaps). If this information is not available, the procedure explained in Annex 2 can be used, in which the size and number of gaps per square meter of the GSC-structure (in front view) can be derived. Two gaps per container. The hydraulic diameter of each gap is equal to $0.16h_{GSC}$, where h_{GSC} is the height of the filled container.

ii. Calculate the hydraulic head at the entrance of each gap and consider the gap as a triangular pipe. Since the head is the difference between the water level behind and after the structure, and the water level up and down stream of the structure is unknown, the head can be calculated by assuming that the water level downstream is zero. This assumption might over predict slightly the permeability of the structure.

iii. Determine the velocity at the entrance of the gap (Bernoulli's equation).

iv. Determine, whether the flow in the gap is turbulent or laminar.

v. For laminar flow, calculate the pipe-friction factor λ using equation 8.

vi. For turbulent flow, calculate the friction factor λ using a roughness value of k_{frc}=0.6mm (k_{fric}=0.0006m) and equation 13, 14 or 15 depending on the flow regime.

vii. Calculate the total friction head loss at each of the individual gap-pipes, using equation 8.

viii. Obtain the velocities at the end of the pipe-gap (Bernoulli's equation) and thus, the total flow in each pipe.

ix. Sum up the flow in each of the pipe-gaps to obtain the total flow through the structure.

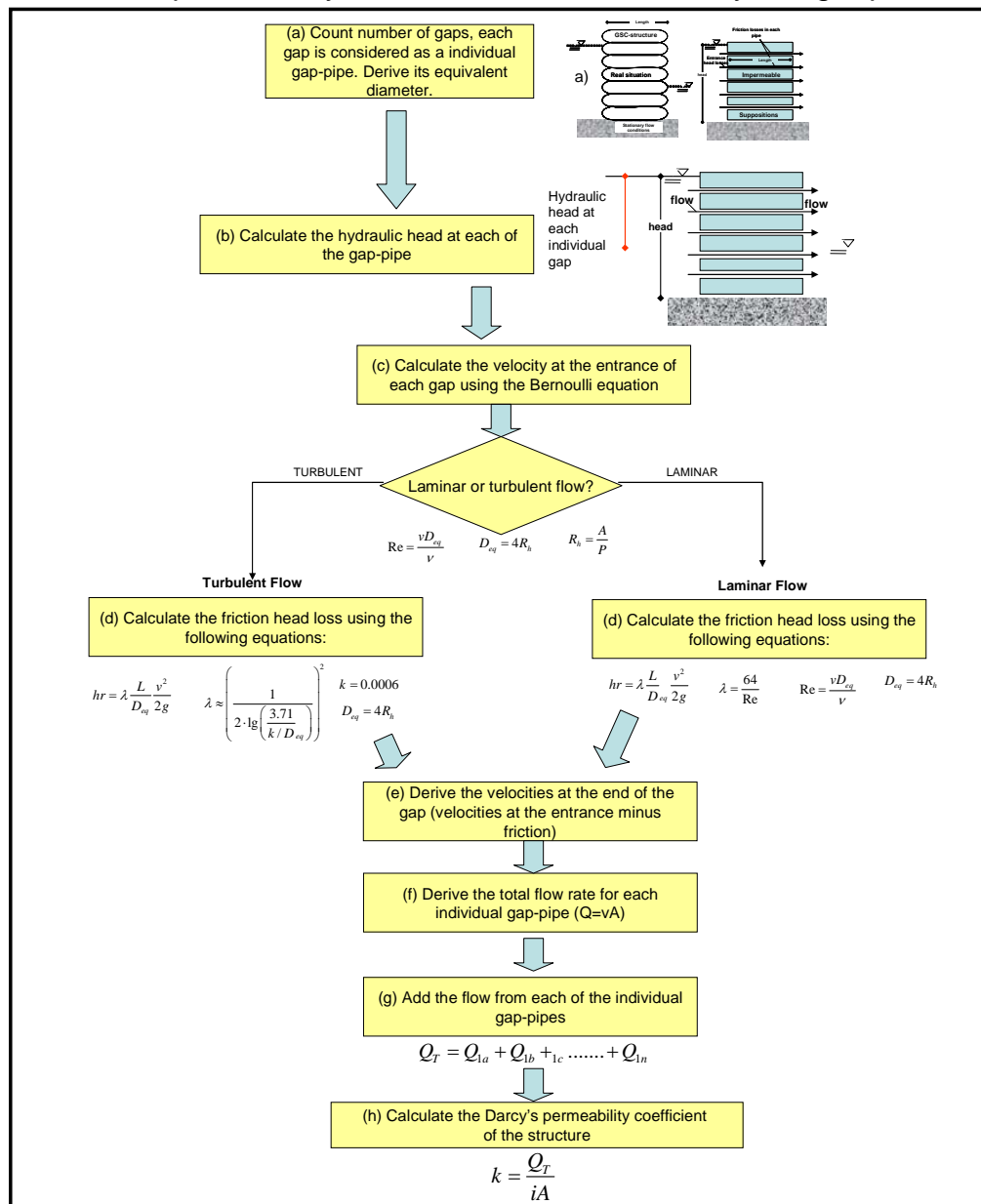x. Calculate the permeability coefficient of the structure by using equation 1

Figure 28: Procedure for the Determination of the Darcy's Permeability Coefficient for GSC-Structures

A "MatLab" programme, which allows to determine the permeability of a GSC-structure based on parameters such as the size of the container used, the water level upstream and dimensions of the structure, is given in Annex 3.

Limitations of the Conceptual Model:
  (i) Due to the limitations of the model tests, only Reynolds numbers between $10^4 < Re < 10^5$ were used. Therefore, higher Reynolds numbers might affect the accuracy of the conceptual model.
  (ii) This procedure should be used for preliminary assessment only, permeability tests should be performed when very accurate permeability coefficients are needed.

8. Summary and Concluding Remarks

Recalling that the filling ratio inside the sand containers was always around 80%, the main results achieved in this report can be summarized as follows:

(i) The permeability of a GSC-structure depends mainly on the size of the gaps. The flow through a GSC-structure is governed by flow through the gaps and thus, the flow through the sand container can be neglected.

(ii) If no reliable data are available, a permeability coefficient for GSC-structures of $k = 10^{-2}$ *m/s* would be reasonable.

(iii) The optimal arrangement to reduce the permeability of a GSC-structure is by blocking the gaps of the first layer with transversal containers of a second layer (see models 7 and 11 in Figure 4 and Table 2). With this mode of placement the permeability coefficient is approximately $k = 5 \times 10^{-3} m/s$.

(iv) The mode of placement of the sand containers in a GSC-structure considerably affects the permeability of the structure. Random placing has the highest permeability, but smaller hydraulic stability for surface piercing structures than longitudinally placed containers.

(v) A simple conceptual model is proposed (section 5), which can be used to approximately estimate the permeability of GSC-structures.

(vi) The pipe-friction roughness was derived from the experiments and found to be around $k_{fric} = 0.6mm$.

Annexes
Annex 1: Procedure to Determine the Number of Gaps and Their Hydraulic Diameter in a GSC-Structure.
Annex 2: Roughness of Different Materials.
Annex 3: MatLab Program to Determine the Permeability of GSC-Structures.

Acknowledgements

References

Aberg B. 1992, Hydraulic Conductivity of Noncohesive Soils. Journal of Geotechnical Engineering 118(9) pages 1335-1347.

Bourzaev Anatoly, 2003, Hydraulische Prozesse an und in einem Deckwerk aus Geotextilen Sandcontainern, Diplom-Arbeit LWI, TU Braunschweig, Germany (in German).

Chao-Lung T. Ming-Chung L. and Chih-Yuan, 2004 „Porosity Effects on Non-breaking Surface Waves over Permeable Submerged Breakwaters. Coastal Engineering Journal, Elsevier, Vol. 50 Issue 4, pages 213-224.

Engelund F. 1953 On the Laminar and Turbulent flows of Groundwater Through Homogeneous Sand. Trans Danish Academy of Technical Sciences, Vol. 3.,

Grüne J., Sparboom U., Schmidt-Koppenhagen R., Wang Z., Oumeraci H., 2006, Stability Tests of Geotextile Sand containers for Monopile Scour Protection, Proceedings of the 30th International Conference of Coastal Engineering, Sand Diego, U.S. (in Print)

Hinz M., Bleck M., and Oumeraci H., 2002, Großmaßstabliche Untersuchungen zur Hydraulischen Stabilität geotextiler Sandcontainer unter Wellenbelastun. LWI-Report no. 878. Leichtweiss Institute, Germany

Hendar P. A. 1960, „Stability of Rock-fill "breakwaters" PhD Thesis, Chalmers Univ. of Technology. Dept. of Hydr. Göteborg, Sweden.

Hudson, R. 1959 Laboratory Investigation of Rubble-Mound Breakwaters. Journal of the Waterways and Harbour Division, pp. 93-118.

Hudson R. Y. 1961, "Laboratory Investigation of Rubble Mound Breakwater" Trans. ASCE 126; 492-541.

Lambe T. W., Whitman R.V., 1979, Soil Mechanics, John Wiley & Sohns, MIT, USA

Liu P. 2004, A finite volume/volume of fluid method for solving the navier-stokes-equation with application to water-wave problems, Lecture Notes of the 3 Days Compact Course, LWI, Germany.

Liu P.L.-F and Lin P., Chang K., Sakakiyama T., 1999, Numerical Modelling of Wave Interaction with Porous Structures. Journal of Waterway, Port, Coastal and Ocean Engineering, ASCE 125 (6)m pages 322-330.

Maricopa County Department of Emergency Management, 2004, Flood Protection, Brochure, USA

Michioku K., Maeno S., Furuzawa T., Haneda M., 2005, Discharge through a Permeable Rubble Mound Weir, Journal of Hydraulic Engineering ASCE, January 2005, pages 1-10.

Muttray M. and Oumeraci H., 2002, Wave Transformation at Sloping Perforated Walls, Proceedings of the International Conference on Coastal Engineering 2002, pages 2031-2043.

Naue Fasetechnik 2004, Secutex GRX, Technical Brochure (in German)

Oumeraci 1999, Hydromechanik, Vorlesungsumdruck für das Grundfach „Hydromechanik", TU-Braunschwieg (in German).

Oumeraci 2002, Küsteningenierwesen, Vorlesungsumdruck für das Vertiefung „Küsteningenierwesen", TU-Braunschwieg (in German).

Pilarczyk K. 1998, Dikes and Revetments, design, maintenance and safety assessment, A.A. Balkema, Rotterdam, the Netherlands

Pilarczyk, K. W. (2000) Geosynthetics and Geosystems in Hydraulic and Coastal Engineering. A.A. Balkema, Rotterdam, ISBN 90 5809 3026, the Netherlands.

Pilarczyk, K. W. 2000 Geosynthetics and Geosystems in Hydraulic and Coastal Engineering. A.A. Balkema, Rotterdam, ISBN 90 5809 3026, the Netherlands.

Porraz M.J.L., Masa A. J. A. and Medina, R.R. 1979, Mortar-filled Containers, Lab and ocean experiences. Proceedings Coastal Structures, pages 270-289.

Recio J., 2004. Hydraulic Processes on GSC-Revetments, Short Progress Report, LWI (internal report).

Recio J., Oumeraci H. 2004. Analyse der stabilitätsgefährdenden Prozesse von GSC-Deckwerken, FZK 2004 pag 83-88

Recio J. and Oumeraci H. 2005, Experimental Results obtained from Model Tests, Wave-induced Forces, PIV visualization and Internal Movement of Sand of a Revetment made with Geotextile Sand Containers, Leichtweiß Institute for Hydraulic Engineering, Progress Report.

Restall S., Hornsey W., Oumeraci H., Hinz M., Saathoff F., and Werth K., 2004, Australian and German Experiences with geotextile Containers for Coastal Protection, proceedings Eurogeo 2004

Sawaragi T., Deguchi I., 1992, Waves on Permeable Layers, Proceedings of the International Conference on Coastal Engineering, pages 1531-1544

Scheidegger A.E. 1974, The Physics of Flow Through Porous Media, University of Toronto Press, Toronto.

Sulisz W., 1995 Effect of Permeability on Stability of rubble Bases. Journal of Waterway, Port, Coastal and Ocean Engineering, May/June 1995 pages 162-170.

Sellers R. 2000, Fluid Mechanics, On-line Lecture Notes, Queen University, Canada (http://me.queensu.ca/courses/MECH241/piping_losses.htm)

Tekmarine Inc. 1982, Large-scale model studies of artic island slope protection. Sierra California.

Vafai K. 2000 Handbook of Porous Media, Marcel Dekker, New York.

Van Gent M. R. A., Tönjes P., Petit H., van den Bosch P. 1994, wave Action on and in Permeable Structures. Proceedings of the international Conference of Coastal Engineering 1994. pages 1739-1753.

Venis, W.A. 1967, Closure of estuarine channels in tidal regions, Behaviour of dumping material when exposed to currents and wave action. De Ingenieur Vol. 50.

Williams AF Burcharth HF and Adel H, 1992, The Permeability of Rubble Mound Breakwaters. New Measurements and New Ideas. Proceedings of the international Conference of Coastal Engineering 1992.

Annex 1
Permeability of GSC-structures
-Derivation of Size of Gap between GSCs from the Size of a GSC-

In this annex, a simple procedure for deriving the size of the gap and its hydraulic diameter is presented. The size of the gap and hydraulic diameter of the gap are needed if the permeability coefficient of a GSC-structure is planned to be derived based on the procedure proposed in Section 7 of this report. The procedure is based on containers that are placed longitudinally as shown in Figure A1-a.
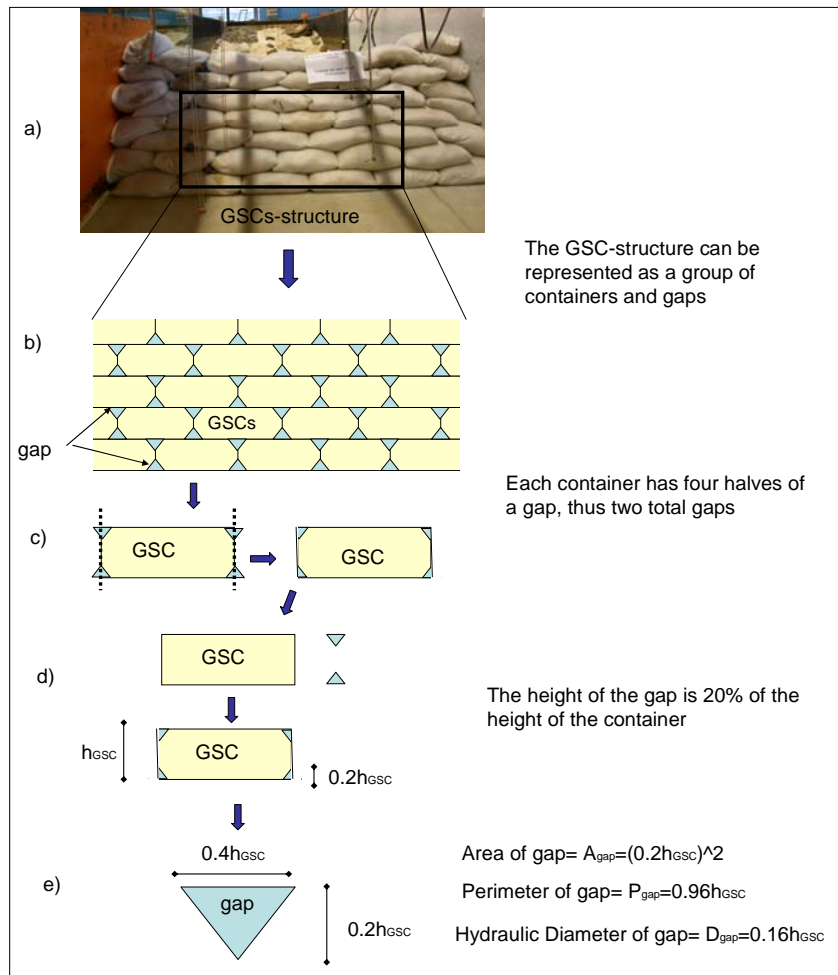

Figure A-1: Derivation of the Gap Parameters from the Size of the Container

For deriving a relation between the size of the container and the gap, three different GSC-structures with different size of container were built and the size of the gap was measured. It was found that:

(i)   In a GSC-structure, each container contributes to four halves of gaps, therefore each container contributes with two gaps to the structure (figure A-1c).

(ii) The height of the gap is approximately 20% of the height of the container h_{GSC}, thus $h_{gap}=0.2h_{GSC}$ (Figure A-1d).

(iii) The hydraulic diameter of the gap D_{Hgap} can be defined by the following equation: $D_{Hgap}= 4A/P$, where A is the area of the gap and P is the perimeter of the gap. The Area of the gap is $0.04h_{GSC}^2$ and the Perimeters is $0.96 h_{GSC}$, thus, the hydraulic diameter of the gap is $D_{Hgap}=0.16h_{GSC}$ (figure A-1e).

(iv) If we used the relation that the length of the container is twice the width and that the height is five times the length then the hydraulic diameter of the gap is $D_{Hgap}=0.16h_{GSC}=0.32 l_{GSC}$.

Annex 2
Permeability of GSC-structures
-Table of Rougness values (k_{fric}) of Several Materials-

This annex shows a table for various roughness of several materials. The table was obtain from (http://www.engineeringtoolbox.com/surface-roughness).

Table 1: Rougness Values (k_{fric}) of Several Materials

Surface	Roughness Coefficients- k	
	millimeters	feet
Copper, Lead, Brass, Aluminum (new)	0.001 - 0.002	$3.33 - 6.7 \ 10^{-6}$
PVC and Plastic Pipes	0.0015 - 0.007	$0.5 - 2.33 \ 10^{-5}$
Stainless steel	0.015	$5 \ 10^{-5}$
Steel commercial pipe	0.045 - 0.09	$1.5 - 3 \ 10^{-4}$
Stretched steel	0.015	$5 \ 10^{-5}$
Weld steel	0.045	$1.5 \ 10^{-4}$
Galvanized steel	0.15	$5 \ 10^{-4}$
Rusted steel (corrosion)	0.15 - 4	$5 - 133 \ 10^{-4}$
New cast iron	0.25 - 0.8	$8 - 27 \ 10^{-4}$
Worn cast iron	0.8 - 1.5	$2.7 - 5 \ 10^{-3}$
Rusty cast iron	1.5 - 2.5	$5 - 8.3 \ 10^{-3}$
Sheet or asphalted cast iron	0.01 - 0.015	$3.33 - 5 \ 10^{-5}$
Smoothed cement	0.3	$1 \ 10^{-3}$
Ordinary concrete	0.3 - 1	$1 - 3.33 \ 10^{-3}$
Coarse concrete	0.3 - 5	$1 - 16.7 \ 10^{-3}$
Well planed wood	0.18 - 0,9	$6 - 30 \ 10^{-4}$
Ordinary wood	5	$16.7 \ 10^{-3}$

Annex 3
Permeability of GSC-Structures
-MatLab Routine for Calculating the Permeability Coefficient of GSC-Structures-

This annex shows the Mat alb routine that calculates the permeability coefficient of structures made of geotextile sand containers (GSC).

When running, the program will ask for the following parameters:
  a) Length of GSC in the direction of flow

  b) Width of GSC

  c) Height of GSC

  d) Length of the GSC-Structure

  e) Height of the GSC-Structure

  f) Width of the GSC-Structure

  g) Water level in front of the GSC-structure

With these parameters the program will calculate and will show on the screen the Darcy's permeability coefficient (k).

The code of the MatLab routine is in the following pages.

Annex 3. Permeability Report

```matlab
                       %ANNEX 3
      % MATLAB ROUTINE FOR CALCULATIING THE PERMEABILITY OF STRUCTURES
             %MADE OF GEOTEXTILE SAND CONTAINERS (GSC)


% program that calculates the permeability of GSC-structures based on the
% dimensions of the GSC-container, the dimensions of the structure and the
% hydraulic gradient at the beginning of the structures.

% the program is based on the conceptual model described in the report by
% Recio and Oumeraci 2007, Permeability of GSC-structures


clear all;
close all;
clc;


'PROGRAM THAT CALCULATES THE PERMEABILITY OF GSC-STRUCTURES'
% we ask for the input parameters


%length of GSC in flow direction
GSClen = input('length of GSC in flow direction ? (m): ');
%GSClen=0.48;


%width of GSC normal to the flow
GSCwid= input('width of GSC normal to the flow ? (m): ');
%GSCwid=0.25;


%height of GSC
GSChei= input('height of GSC in front view ? (m): ');
%GSChei= 0.11;


%length of structure in flow direction
StrLen= input('lengtht of GSC-structure in flow direction ? (m): ');
%StrLen= 0.48;


%width of structure
StrWid= input('width of GSC-structure normal to flow ? (m): ');
%StrWid=2;


%structure heigth
StrHei= input('height of GSC-structure in front view ? (m): ');
%StrHei=1;


%water level infront of GSC-structure
WL= input('water level infront of GSC-structure in front view ? (m): ');
%WL=0.80;


%we calculate hydraulic diameter of the gap
D=0.16*GSChei;


%roughnes of gappipe
k=0.0006;


%area of gap, based on annex 1 of permeability report
A=(0.2*GSChei)^2;


%number of containers in width
NuGSCwid= round(StrWid/GSCwid);


%number of containers in height
NuGSChei=round(WL/GSChei);
```

Annex 3. Permeability Report

```matlab
%matrix with the hydraulic head in each of the vertical gaps starting with
%gap at the bottom
mm= NuGSChei;
j=1;
for j=1:mm;
    Hhead(j)=WL-(j*GSChei);
end


%matrix with velocity at the entrance
j=1;
for j=1:mm;
    VelIni(j)=(2*9.81*Hhead(j))^0.5;
end


%matrix with reynolds number
j=1;
for j=1:mm;
    ReNum(j)=(VelIni(j)*D/.000001);
end


% we calculate friction loss in each pipe depending if it is turbulent or
% laminar
j=1;
for j=1:mm;
    if ReNum(j)<10000; % then flow is laminar
    if ReNum(j)==0;% to avoid dividing by zero
        ReNum(j)=100;
    end
        FriFac(j)=[64/ReNum(j)];
    end

    if ReNum(j)>10000; %then  flow is turbunel
        FriFac(j)=[1/[2*log(3.71/(k/D))]]^2;
    end
end


% we calculate velocity at the end of the gap
j=1;
for j=1:mm;
    Hr(j)=FriFac(j)*[(StrLen*(VelIni(j)^2))/(D*2*9.91)];
    Auxi1(j)=[VelIni(j)^2]/(2*9.81);
    VelEnd(j)=abs([[Auxi1(j)-Hr(j)]*2*9.81])^0.5;
end


% we obtain the flow rate in each of the gaps
j=1;
for j=1:mm;
    Qgap(j)=VelEnd(j)*A;
end


% we multiply for eah number of gaps that are in the same heigth

%horizontal gaps per layer
Auxi2=round(StrWid/GSCwid);%
%flow rate on each layer
j=1;
for j=1:mm;
    Qlayer(j)=Qgap(j)*Auxi2;
end


%we add the flow from each layer and get the total flow

j=1;
```

Annex 3. Permeability Report

```
Qtot=0;
for j=1:mm;
    Qaux=Qlayer(j);
    Qtot=Qtot+Qaux;
end

'the total flow throught the Structure is (m3/s)='
Qtot

%permeability coefficient
Astr=StrWid*WL;
Dl=[(WL/2)^2+StrLen^2]^0.5;
i=WL/Dl;
kf=Qtot/(i*Astr);
'permeability coefficient of the structure (m/s)='
kf
```